Cancer Science
The official journal of the Japanese Cancer Association JCA

Phase II study of oral fludarabine in combination with rituximab for relapsed indolent B-cell non-Hodgkin lymphoma

Kensei Tobinai,[1,16] Ken-ichi Ishizawa,[2] Michinori Ogura,[3] Kuniaki Itoh,[4] Yasuo Morishima,[6] Kiyoshi Ando,[7] Masafumi Taniwaki,[8] Takashi Watanabe,[1] Joji Yamamoto,[2] Toshiki Uchida,[3] Masanobu Nakata,[4,13] Takashi Terauchi,[9] Shigeru Nawano,[5,14] Masaki Matsusako,[10] Masaki Hayashi[11,15] and Tomomitsu Hotta[12]

[1]Hematology and Stem Cell Transplantation Division, National Cancer Center Hospital, Tokyo; [2]Hematology and Rheumatology, Tohoku University Hospital, Sendai; [3]Department of Hematology and Oncology, Nagoya Daini Red Cross Hospital, Nagoya; Divisions of [4]Oncology and Hematology, and [5]Diagnostic Radiology, National Cancer Center Hospital East, Chiba; [6]Department of Hematology and Cell Therapy, Aichi Cancer Center Hospital, Nagoya; [7]Department of Hematology and Oncology, Tokai University School of Medicine, Kanagawa; [8]Department of Hematology and Oncology, Kyoto Prefectural University of Medicine, Kyoto; [9]Screening Technology and Development Division, Research Center for Cancer Prevention and Screening, National Cancer Center, Tokyo; [10]Department of Radiology, St Lukes International Hospital, Tokyo; [11]Department of Clinical Development, Bayer HealthCare, Osaka; [12]Nagoya Medical Center, Nagoya; [13]Department of Internal Medicine, Sapporo Hokuyu Hospital, Sapporo; [14]Department of Radiology, International University of Health and Welfare Mita Hospital, Tokyo; [15]Department of Internal Medicine, Nakagami Hospital, Okinawa, Japan

(Received April 10, 2009/Revised May 24, 2009/Accepted May 30, 2009/Online publication July 7, 2009)

Oral fludarabine is more convenient than intravenous fludarabine in an outpatient setting. To assess the efficacy and toxicity of oral fludarabine in combination with rituximab in patients with relapsed indolent B-cell non-Hodgkin lymphoma (B-NHL), we conducted a multicenter phase II study. Patients with relapsed indolent B-NHL with two or fewer prior regimens and up to 16 doses of rituximab were eligible. Patients received 375 mg/m² rituximab on day 1, and 40 mg/m² oral fludarabine once daily on days 1 through 5 every 28 days for up to six cycles. The primary endpoint was the overall response rate. Forty-one patients were enrolled, including 38 (93%) with follicular lymphoma. Thirty-four patients (83%) had received rituximab as prior therapy. Twenty-seven patients (66%) completed the planned six cycles. Dose reduction of oral fludarabine was required in 17 patients (41%). The overall response rate was 76% (31 of 41 patients; 95% confidence interval, 60–88%) with a complete response rate of 68% (28 of 41 patients; 95% confidence interval, 52–82%). Median progression-free survival for the 41 patients was 19.7 months (95% confidence interval, 12.3–26.5 months). Hematological toxicities, including grade 4 neutropenia (68%), were the most frequent toxicities. Non-hematological toxicities were mild, except for one patient who died of *Pneumocystis jiroveci* pneumonia 4 months after the protocol treatment. In conclusion, oral fludarabine in combination with rituximab is a highly effective and convenient therapy for patients with relapsed indolent B-NHL who have mostly been pretreated with rituximab. (ClinicalTrials.gov number, NCT00311129.) (*Cancer Sci* 2009; 100: 1951–1956)

Indolent B-cell non-Hodgkin lymphoma (B-NHL), mainly consisting of follicular lymphoma, has a long course of disease, usually requiring multiple treatment regimens.[1] Although a recent meta-analysis of seven randomized studies for previously untreated and treated indolent B-NHL confirmed a survival benefit associated with the addition of rituximab to chemotherapy,[2] no standard chemotherapy regimens have been established. Among various combination chemotherapy regimens, cyclophosphamide, doxorubicin, vincristine, and prednisone (CHOP) chemotherapy, and cyclophosphamide, vincristine, and prednisone (CVP) are frequently used regimens in combination with rituximab;[3–6] however, they have certain limitations, including peripheral neuropathy, alopecia, and cardiac toxicity. In addition, recent reports regarding the long-term follow-up results of CVP and CHOP in combination with rituximab for indolent B-NHL revealed that these regimens are not satisfactory in view of long-term response durability.[6,7] Thus, novel combinations with highly effective and less-toxic profiles are required. Most patients with indolent B-NHL have a good performance status, which makes outpatient treatment desirable. Effective oral treatment in combination with rituximab may decrease the number of clinic visits and reduce the consumption of medical resources.

Fludarabine phosphate is one of the most effective drugs in the treatment of indolent B-NHL,[8,9] and exhibits a better progression-free survival (PFS) than CVP.[10] To improve the efficacy of fludarabine as a single agent, a variety of combination therapies has been reported, including fludarabine plus cyclophosphamide,[11] and fludarabine plus mitoxantrone and dexamethasone.[12,13] Despite the excellent antitumor activities of these combinations, long-lasting myelosuppression and increased risk of opportunistic infections are clinically significant problems.[14–16]

Several preclinical studies suggested the potential synergism between fludarabine and rituximab.[17–19] In addition, rituximab has been shown *in vitro* to sensitize drug-resistant lymphoma cell lines to cytotoxic chemotherapy.[20] Intravenous fludarabine in combination with rituximab was reported to be effective in the treatment of treatment-naïve or relapsed patients with indolent B-NHL, with 90% overall response rate (ORR).[21] Although the combination is very effective, intravenous administration of fludarabine for 5 consecutive days is inconvenient in an outpatient setting. We reported the results of phase I and II studies of oral fludarabine in relapsed indolent B-NHL previously.[22,23] As a single agent for relapsed patients who have been mostly pretreated with rituximab, it showed the ORR and complete response (CR) rates of 65 and 30%, respectively.[23] To further enhance the effectiveness of oral fludarabine, we conducted a multicenter phase II study to evaluate the efficacy and safety of oral fludarabine in combination with rituximab for relapsed indolent B-NHL.

Patients and Methods

Patient selection. Patients aged 20–74 years, with relapsed or refractory, histologically confirmed CD20-positive, indolent B-NHL (World Health Organization classification: small lymphocytic lymphoma, lymphoplasmacytic lymphoma, splenic marginal zone B-cell lymphoma, extranodal marginal zone B-cell lymphoma of mucosa-associated lymphoid tissue type, nodal marginal zone

[16]To whom correspondence should be addressed. E-mail: ktobinai@ncc.go.jp

doi: 10.1111/j.1349-7006.2009.01247.x

B-cell lymphoma, and follicular lymphoma) were eligible.[24] Patients with mantle cell lymphoma were excluded. Patients were to have measurable disease, an Eastern Cooperative Oncology Group performance status of 0–1,[25] an expected survival of more than 3 months, and no major organ dysfunctions (neutrophil counts $\geq$ 1500/μL, peripheral blood tumor cells < 5000/μL, platelet counts $\geq 7.5 \times 10^4$/μL, aspartate aminotransferase and alanine transaminase (ALT) < 2.5 × upper limit of normal, total bilirubin < 1.5 × upper limit of normal, serum creatinine < 1.5 × upper limit of normal, and no electrocardiogram (ECG) abnormalities requiring treatment). The number of prior chemotherapy regimens was limited to two or fewer, and prior rituximab treatments up to 16 times were allowed, but the duration from the last treatment had to be at least 4 weeks for chemotherapy and 6 months for rituximab. The following exclusion criteria were applied: positivity of hepatitis B virus surface antigen, hepatitis C virus antibody, or human immunodeficiency virus antibody, infectious disease, other serious complications, history of autoimmune hemolytic anemia, prior hematopoietic stem cell transplantation, and prior therapy with fludarabine, pentostatin, or cladribine. Patients with active other malignancies requiring treatment were also excluded. Pregnant or lactating women were not eligible, and all patients were required to use contraception as necessary. The study protocol was approved by the institutional review board of each participating institution before the patients were enrolled in the study. All patients gave written informed consent before they entered the study.

Study design and protocol treatment. This was a non-randomized phase II study. Rituximab (provided by Zenyaku Kogyo, Tokyo, Japan) at 375 mg/m^2 was intravenously administered on day 1 of each treatment cycle along with oral dosing of 40 mg/m^2 fludarabine phosphate tablets once daily from day 1 through 5 every 28 days for up to six cycles. Rituximab dosage was fixed throughout the course, and was infused according to the package insert. At the end of each cycle, adverse events were assessed, and the start of the next cycle and the dosage of fludarabine phosphate tablet were determined. If a patient developed toxicities on certain treatment days, the treatment was postponed, or the dosage of oral fludarabine was reduced to 30 mg/m^2 daily for all subsequent cycles. In addition, the dosage of oral fludarabine was reduced to 30 mg/m^2 daily if severe toxicities were observed during the treatment cycles. If postponement lasted longer than 14 days, the protocol treatment was terminated. Prophylactic use of trimethoprim and sulfamethoxazole and acyclovir was recommended, and granulocyte colony-stimulating factor (G-CSF) was given as needed.

Patient monitoring. Patients were admitted for the first infusion of rituximab to observe its infusion-related toxicities, but thereafter they could be treated as outpatients. The following evaluations were carried out during the pretreatment screening period: vital signs, ECG, laboratory studies, human antichimera antibody, bone marrow aspiration or biopsy with nested PCR for immunoglobulin heavy-chain and *bcl-2* gene (IgH/*bcl-2*) rearrangement, and computed tomography (CT) imaging. During the treatment, patients were observed by physical examination, complete blood counts, and serum chemistry every week. CT scan and bone marrow aspiration or biopsy were carried out 4 weeks after the start of the third and sixth courses in patients who showed positive lymphomatous lesions before enrolment. If baseline bone marrow IgH/*bcl-2* gene rearrangement was positive and the patient achieved a partial or better response, bone marrow PCR for IgH/*bcl-2* gene rearrangement was repeated. Patients were observed until 12 weeks after completion of the protocol treatment or until the assessment of progressive disease (PD); thereafter, the patients were followed up regularly until PD or death.

Data analysis. Responses were assessed according to the International Workshop Criteria for non-Hodgkin lymphoma as follows.[26] CR required the complete disappearance of all lesions and radiological or biological abnormalities and the absence of new lesions. CR unconfirmed described patients who met the criteria of CR but who had an indeterminate bone marrow assessment or a more than 75% decrease from baseline in the sum of the products of the greatest perpendicular diameters (SPD) of all measurable lesions but with a residual mass. Partial response was defined as a more than 50% decrease from baseline in the SPD of all measured lesions, no increase in the size of any other lesions, and no new lesions. Stable disease was defined as neither a 50% decrease nor a 50% increase in the SPD of measured lesions, and PD was defined as the appearance of any new lesion or a more than 50% increase in the SPD from nadir. Confirmation of response by repeat measurement 28 or more days later was not required. In addition to the efficacy evaluation at each participating institute, an independent, third-party panel of three radiologists (T.T., S.N., and M.M.) carried out a central evaluation using the collected CT films. The primary efficacy variable was best ORR (the relative frequency of responders showing CR, CR unconfirmed, or partial response). Secondary efficacy variables included CR rate, PFS (defined as the time from the date of enrollment to the date of PD assessment, the date of death of any cause, or the date necessitating other antilymphoma treatment), and overall survival (defined as the period from the date of registration to the date of death due to any cause).

Safety variables for the study were the types, incidence, severity, and reversibility of adverse events and adverse drug reactions, changes in laboratory tests, and the proportion of dose reduction. Toxicity was graded according to the Common Terminology Criteria for Adverse Event v3.0. Follicular Lymphoma International Prognostic Index (FLIPI) scores were calculated by summing the number of risk factors (age > 60 years, Ann Arbor stage III or IV, hemoglobin < 12 g/dL, elevated lactate dehydrogenase, and >4 nodal areas).[27] The following three risk groups were defined: low (none or one risk factor), intermediate (two risk factors), and poor risk (three to five risk factors).

Statistical methods. The study was designed to detect an expected ORR of 75%, assuming a threshold ORR of 50%. The level of significance was set at 2.5% (one-tailed) and the required sample size to attain statistical power of 80% was 35 patients. The target number of patients for registration was set at 40 patients, assuming that up to 15% of the enrolled patients might be judged unassessable. The Kaplan–Meier method was used to analyze survival probabilities.

Results

Patient characteristics. Between December 2005 and October 2006, 41 patients with relapsed or refractory indolent B-NHL were enrolled from seven institutions. Table 1 summarizes the patient characteristics. The majority of patients (93%) had follicular lymphoma, and 61% of patients had advanced-stage diseases upon entering the study. FLIPI risk groups were low in 25 (61%), intermediate in 11 (27%), and high in five patients (12%). Thirty-four patients (83%) had received rituximab before entering the study.

Protocol treatment. Of the 41 patients enrolled, 27 (66%) completed the planned six cycles of protocol treatment. The protocol treatment was terminated because of progression of the primary disease in two patients (5%), and due to adverse events in 12 (29%; neutropenia in five, neutropenia and thrombocytopenia in two, thrombocytopenia in three, hemolytic anemia in one, and withdrawal of consent due to anorexia in one). The dose reduction of oral fludarabine to 30 mg/m^2/day according to the protocol-defined criteria was required in 17 patients (41%). The dose was reduced during the second course in one, third in six, fourth in three, fifth in four, and sixth in three patients.

Efficacy. The efficacy results are summarized in Table 2. The ORR and CR rates were 76% (95% confidence interval [CI], 60–88%) and 68% (95% CI, 52–82%), respectively; and 25 (74%) of the 34 patients who had received prior rituximab

doi: 10.1111/j.1349-7006.2009.01247.x

responded to the combination. The CR rates correlated with the risk groups according to the FLIPI. The median PFS for all 41 patients was 19.7 months (95% CI, 12.3–26.5 months), and the median PFS for the 31 responders was 20.4 months (95% CI, 16.1–26.5 months) (Fig. 1a). The PFS correlated well with the risk groups according to the FLIPI (Fig. 1b). Sixteen of the 41 patients examined (39%) had positive IgH/*bcl-2* gene rearrangement by PCR in bone marrow at baseline. Of the 16 patients, 14 (88%) became negative by the sixth course, but one became positive again during the follow-up period.

Table 1. Patient baseline clinical characteristics

Characteristic	No. patients	%
All	41	100
Sex		
Male	17	41
Female	24	59
Age (years)		
Median (range)	57 (40–73)	
≤44	4	10
45–64	28	68
≥65	9	22
ECOG performance status†		
0	35	85
1	6	15
Histology (WHO Classification)		
Small lymphocytic lymphoma	1	2
Follicular lymphoma	38	93
Extranodal marginal zone B-cell lymphoma, MALT	2	5
Ann Arbor stage†		
IA	3	7
IIA	13	32
IIIA	10	24
IVA	15	37
FLIPI*		
Low	25	61
Intermediate	11	27
High	5	12
Prior therapy		
Rituximab monotherapy	9	22
Chemotherapy with rituximab	25	61
Chemotherapy without rituximab	7	17

ECOG, Eastern Cooperative Oncology Group; FLIPI, Follicular Lymphoma International Prognostic Index; MALT, mucosa-associated lymphoid tissue; WHO, World Health Organization.
†At study entry.

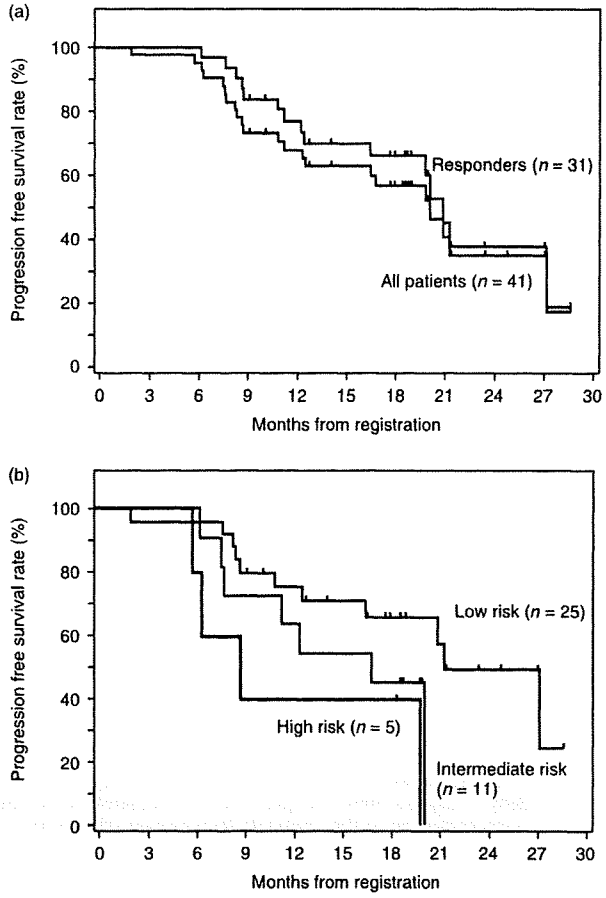

Fig. 1. Progression-free survival (PFS) of patients with relapsed indolent B-cell non-Hodgkin lymphoma who were treated with oral fludarabine and rituximab. (a) PFS of 41 patients and 31 responders. (b) PFS according to Follicular Lymphoma International Prognostic Index (FLIPI): low risk ($n = 25$), intermediate risk ($n = 11$), and high risk ($n = 5$).

Table 2. Antitumor effect of oral fludarabine and rituximab

Treatment group	No. patients	No. patients						ORR		CR rate	
		CR	CRu	PR	SD	PD	NE	%	95% CI	%	95% CI
All	41	22	6	3	6	2	2	76	60–88	68	52–82
FL	38	21	6	1	6	2	2	74		71	
MALT	2	0	0	2	0	0	0	100		0	
SLL	1	1	0	0	0	0	0	100		100	
Prior rituximab†											
+	34	17	6	2	6	2	1	74		68	
–	7	5	0	1	0	0	1	86		71	
FLIPI											
Low	25	15	5	0	3	1	1	80		80	
Intermediate	11	6	0	3	1	1	0	82		55	
High	5	1	1	0	2	0	1	40		40	

Responses were assessed according to the International Workshop Response Criteria for Non-Hodgkin Lymphoma.[26]
CR, complete response; CRu, complete response unconfirmed; FL, follicular lymphoma; FLIPI, Follicular Lymphoma International Prognostic Index; MALT, extranodal marginal zone B-cell lymphoma of mucosa-associated lymphoid tissue; ORR, overall response rate; PD, progressive disease; PR, partial response; SD, stable disease; SLL, small lymphocytic lymphoma.
†+ and – indicate the presence and absence of prior rituximab treatment, respectively.

Table 3. Incidence of hematological and non-hematological toxicities observed in 20% or higher of 41 patients

Toxicity	Any grade		Grade 3		Grade 4	
	No. patients	%	No. patients	%	No. patients	%
Leukopenia	41	100	21	51	17	41
Neutropenia	40	98	11	27	27	66
Lymphopenia	41	100	1	2	40	98
Erythropenia	34	83	4	10	1	2
Thrombocytopenia	28	68	6	15	3	7
Anemia	27	66	5	12	2	5
Monocytopenia	27	66	0	0	0	0
LDH elevation	29	71	0	0	0	0
AST elevation	20	49	2	5	0	0
ALT elevation	16	39	3	7	0	0
IgM decrease	15	37	1	2	1	2
IgA decrease	10	24	1	2	1	2
IgG decrease	10	24	1	2	1	2
Hypoproteinemia	10	24	1	2	0	0
Creatinine elevation	9	22	1	2	0	0
Hyperbilirubinemia	9	22	0	0	0	0
Nausea	25	61	0	0	0	0
Anorexia	17	41	0	0	0	0
Stomatitis	13	32	0	0	1	2
Malaise	13	32	0	0	0	0
Pyrexia	13	32	0	0	0	0
Vomiting	12	29	2	5	0	0
Diarrhoea	11	27	1	2	0	0
Headache	11	27	0	0	0	0
Nasopharyngitis	11	27	0	0	0	0
Back pain	9	22	0	0	0	0
Chills	9	22	0	0	0	0
Constipation	9	22	0	0	0	0

ALT, alanine transaminase; AST, aspartate aminotransferase; LDH, lactate dehydrogenase. Hematological and non-hematologic toxicities were graded according to the Common Terminology Criteria for Adverse Event v3.0.

Adverse events. Hematological and non-hematological adverse events that were encountered in 20% or more of treated patients are listed in Table 3. Hematological toxicity was common, although it was manageable mostly in the outpatient setting. Grade 4 neutropenia was observed in 27 patients (66%), and grade 4 thrombocytopenia in three (7%). G-CSF of 50–100 μg was subcutaneously given to 10% (4/41) of patients at cycle 1, 24% (10/41) at cycle 2, 33% (13/39) at cycle 3, 36% (13/36) at cycle 4, 45% (15/33) at cycle 5, and 26% (7/27) at cycle 6. The duration of G-CSF administration was 1–3 days in most patients. There were four episodes of grade 3 infection (two with febrile neutropenia, one with cystitis, and one with influenza), with no grade 4 infections during the study. Non-hematological toxicities were generally mild. All non-hematological adverse events of grade 3 or greater were seen in 5% or fewer patients except for ALT elevation (7%). Grade 4 non-hematological toxicities were observed in only two patients (5%; one with stomatitis and immunoglobulin decrease, and one with hyperuricemia).

Eleven serious adverse events (SAE) were observed in nine patients during the study: neutropenia (grade 4, two patients), leukopenia (grade 4, one patient), pancytopenia (grade 4, one patient), hemolytic anemia (grade 2, one patient), febrile neutropenia (grade 3, one patient), creatinine elevation (grade 3, one patient), stomatitis (grade 4, one patient), cystitis (grade 2, one patient), deep vein thrombosis (grade 3, one patient), and gastric cancer (grade 3, one patient). Two SAE in two patients (one with pancytopenia and one with leukopenia) did not recover, and the study was terminated in three patients due to SAE (one due to leukopenia and neutropenia, one due to stomatitis, and one due to hemolytic anemia). In one patient, early gastric cancer was detected during cycle 6, which was successfully treated by endoscopic mucosal resection. After the study, three SAE were reported: one patient each for herpes zoster, pneumonia, and *Pneumocystis jiroveci* pneumonia. In all SAE, a causal relation with the study medications was not ruled out, except for gastric cancer, which was judged as not related to the study treatment.

There were no deaths during the study period; however, three deaths were reported after the completion of the study. Two were from lymphoma progression, but one patient died of *Pneumocystis jiroveci* pneumonia. A 71-year-old woman with follicular lymphoma, previously treated with rituximab plus CHOP chemotherapy, received six courses of oral fludarabine and rituximab. After the sixth course, lymphopenia and pancytopenia persisted. Four months later she developed *Pneumocystis jiroveci* pneumonia and died of respiratory failure. She was on prophylactic trimethoprim and sulfamethoxazole (1 Tab; 80 mg/400 mg daily) when she developed *Pneumocystis jiroveci* pneumonia. The event was considered to be associated with immune suppression caused by the study medications.

There was another episode of *Pneumocystis jiroveci* pneumonia 4 months after completion of six cycles of treatment. The patient was not on prophylactic trimethoprim/sulfamethoxazole after completion of the protocol treatment. This patient was successfully treated with trimethoprim/sulfamethoxazole, along with other supportive medications.

Discussion

This is the first study to document the high efficacy of oral fludarabine in combination with rituximab in patients with relapsed indolent B-NHL. The ORR of 76% and CR rate of 68% are higher than the 65% and 30%, respectively, in our previous phase II study of oral fludarabine alone,[23] although this is not a direct comparison. The efficacy rates by the combination are considered very high, although all patients enrolled in this study had relapsed disease, and the majority of patients had prior treatment with rituximab, either alone or in combination with chemotherapy. In the phase II study by Czuczman *et al.* using intravenous fludarabine plus rituximab, the ORR and CR rate were reported to be 90 and 80%, respectively.[21] In their study, however, the target population was mostly untreated patients (68%), and patients having a history of prior rituximab therapy were excluded.

In addition, the median PFS (19.7 months) obtained with this combination in the present study is promising, comparing with the reported median PFS by other agents in relapsed indolent B-NHL patients, including 8 months with cladribine,[28] 8.6 months with oral fludarabine alone,[23] 8–9 months with rituximab,[29,30] 11.2 months with yttrium-90-labeled ibritumomab tiuxetan,[31] and 23–24 months with bendamustine plus rituximab,[32,33] although the target population is somewhat different among studies. The high efficacy and long PFS suggest that oral fludarabine plus rituximab is a reasonable option in the current treatment of relapsed indolent B-NHL. In addition, considering the favorable efficacy results by the combination of intravenous fludarabine and rituximab for mostly untreated patients with indolent B-NHL,[21] it may deserve to conduct a prospective study of oral fludarabine plus rituximab for untreated indolent B-NHL. To elucidate the exact role of this combination in the treatment of untreated and relapsed indolent B-NHL, further carefully designed studies are required.

In the present study, 14 of the 16 patients (88%) whose bone marrow aspirates showed positive IgH/*bcl-2* gene rearrangement by PCR became negative by oral fludarabine plus rituximab therapy. It is likely that these results are at least equivalent to the 88% (14/16) in the phase II study of intravenous fludarabine plus rituximab for mostly untreated indolent B-NHL patients.[21]

doi: 10.1111/j.1349-7006.2009.01247.x

The most common toxicities were hematological, with grade 4 neutropenia occurring in 66% of patients, which was higher than the 37% with oral fludarabine alone.[23] Intravenous fludarabine in combination with rituximab was reported to have an increased risk of developing grade 3 or greater neutropenia.[21] Although neutropenia was also common in the present study, only four episodes of grade 3 infection were seen, with no grade 4 infections during the study period. In the study of intravenous fludarabine with rituximab,[21] the initial 10 patients showed frequent severe neutropenia, necessitating modifications to reduce the dose in case of prolonged hematological toxicity and omitting prophylactic trimethoprim/sulfamethoxazole. Our study used an approach to reduce the dose if severe hematological toxicities were observed, and allowed the liberal use of G-CSF, while using prophylactic trimethoprim/sulfamethoxazole and acyclovir. It is likely that this approach was effective in reducing infectious episodes. Although the exact mechanism of the higher incidence of neutropenia by the combined use of rituximab and fludarabine than that with fludarabine alone remains unknown, it may be partly associated with the hematological toxicity of rituximab alone[30] and late-onset neutropenia in patients pretreated with rituximab, especially with rituximab-containing chemotherapy.[34] The non-hematological toxicities were infrequent, mild, and mostly manageable.

Of note was that one death from *Pneumocystis jiroveci* pneumonia occurred 4 months after completion of the protocol treatment. Another patient developed *Pneumocystis jiroveci* pneumonia 4 months after completing the sixth course, but recovered with anti-*Pneumocystis* therapy. Fludarabine is known to cause prolonged immunosuppressive effects in view of decreased CD4-positive T-cell counts and decreased serum IgG levels,[16] and rituximab causes prolonged B-lymphocyte suppression.[29,30] These results suggest that prolonged prophylaxis for *Pneumocystis jiroveci* infection is recommended in patients who receive fludarabine plus rituximab, in addition to the careful monitoring of absolute lymphocyte counts and CD4-positive T-cell counts.

In this multicenter phase II study, a central pathology review was not carried out. As the diagnosis of only one of the 52 enrolled patients was changed in the central pathology review in our previous multicenter phase II study of oral fludarabine alone for relapsed indolent B-NHL,[23] we did not consider the central pathology review in this study to be essential.

In conclusion, oral fludarabine in combination with rituximab is a highly effective and convenient treatment for relapsed indolent B-NHL, in view of the high ORR, CR rate, long PFS, and the convenience of administering it in an outpatient setting. Although hematological toxicities appeared to be somewhat higher than with oral fludarabine alone, and dose reduction of oral fludarabine was necessary in a fraction of patients, non-hematological toxicities were generally mild; however, prolonged prophylaxis for *Pneumocystis jiroveci* pneumonia is recommended when using this combination. The encouraging results warrant further investigations of this combination in the treatment of indolent B-NHL, including frontline therapy.

Acknowledgments

We thank the investigators (physicians and staff) at the participating institutions for their help: K. Esaki, MD (Fujita Health University), K. Toyama, MD (Tokyo Medical College), and K. Hatake, MD (The Cancer Institute Hospital of Japanese Foundation for Cancer Research) as members of the Independent Monitoring Committee, and Takeshi Morinaga (Bayer HealthCare).

Disclosure Statement

Masaki Hayashi was an employee of Bayer HealthCare, Osaka, Japan. The remaining authors report no potential conflicts of interest.

References

1 Horning SJ. Natural history of and therapy for the indolent non-Hodgkin's lymphomas. *Semin Oncol* 1993; **20**: 75–88.
2 Schulz H, Bohlius JF, Trelle S *et al.* Immunochemotherapy with rituximab and overall survival in patients with indolent or mantle cell lymphoma: a systematic review and meta-analysis. *J Natl Cancer Inst* 2007; **99**: 706–14.
3 Czuczman MS, Weaver R, Alkuzweny B, Berlfein J, Grillo-López AJ. Prolonged clinical and molecular remission in patients with low-grade or follicular non-Hodgkin's lymphoma treated with rituximab plus CHOP chemotherapy: 9-year follow-up. *J Clin Oncol* 2004; **22**: 4711–16.
4 Hiddemann W, Kneba M, Dreyling M *et al.* Frontline therapy with rituximab added to the combination of cyclophosphamide, doxorubicin, vincristine, and prednisone (CHOP) significantly improves the outcome for patients with advanced-stage follicular lymphoma compared with therapy with CHOP alone: results of a prospective randomized study of the German Low-Grade Lymphoma Study Group. *Blood* 2005; **106**: 3725–32.
5 Ogura M, Morishima Y, Kagami Y *et al.* Randomized phase II study of concurrent and sequential rituximab and CHOP chemotherapy in untreated indolent B-cell lymphoma. *Cancer Sci* 2006; **97**: 305–12.
6 Marcus R, Imrie K, Solal-Celigny P *et al.* Phase III study of R-CVP compared with cyclophosphamide, vincristine, and prednisone alone in patients with previously untreated advanced follicular lymphoma. *J Clin Oncol* 2008; **26**: 4579–86.
7 Itoh K, Igarashi T, Ogura M *et al.* Randomized phase II study of concurrent and sequential combinations of rituximab (R) plus CHOP (R-CHOP) in untreated indolent B-NHL: 7-year follow-up results. *J Clin Oncol* 2008; **26** (Suppl; Abstract 8616): 482s.
8 Hochster HS, Kim KM, Green MD *et al.* Activity of fludarabine in previously treated non-Hodgkin's low-grade lymphoma: results of an Eastern Cooperative Oncology Group study. *J Clin Oncol* 1992; **10**: 28–32.
9 Redman JR, Cabanillas F, Velasquez WS *et al.* Phase II trial of fludarabine phosphate in lymphoma: an effective new agent in low-grade lymphoma. *J Clin Oncol* 1992; **10**: 790–4.
10 Klasa RJ, Meyer RM, Shustik C *et al.* Randomized phase III study of fludarabine phosphate versus cyclophosphamide, vincristine, and prednisone in patients with recurrent low-grade non-Hodgkin's lymphoma previously treated with an alkylating agent or alkylator-containing regimen. *J Clin Oncol* 2002; **20**: 4649–54.
11 Flinn IW, Byrd JC, Morrison C *et al.* Fludarabine and cyclophosphamide with filgrastim support in patients with previously untreated indolent lymphoid malignancies. *Blood* 2000; **96**: 71–5.
12 McLaughlin P, Hagemeister FB, Romaguera JE *et al.* Fludarabine, mitoxantrone, and dexamethasone: an effective new regimen for indolent lymphoma. *J Clin Oncol* 1996; **14**: 1262–8.
13 Tsimberidou AM, McLaughlin P, Younes A *et al.* Fludarabine, mitoxantrone, dexamethasone (FND) compared with an alternating triple therapy (ATT) regimen in patients with stage IV indolent lymphoma. *Blood* 2002; **100**: 4351–7.
14 Hochster HS, Oken MM, Winter JN *et al.* Phase I study of fludarabine plus cyclophosphamide in patients with previously untreated low-grade lymphoma: results and long-term follow-up – a report from the Eastern Cooperative Oncology Group. *J Clin Oncol* 2000; **18**: 987–94.
15 Hochster H, Weller E, Kuzel T *et al.* Increased mortality associated with higher dose cyclophosphamide plus fludarabine in advanced stage indolent lymphoma patients treated on E1496, an ECOG and CALGB study. *Proc Am Soc Clin Oncol* 2002; **21**: 282a.
16 Tsimberidou A-M, Younes A, Romaguera J *et al.* Immunosuppression and infectious complications in patients with stage IV indolent lymphoma treated with a fludarabine, mitoxantrone, and dexamethasone regimen. *Cancer* 2005; **104**: 345–53.
17 Alas S, Emmanouilides C, Bonavida B. Inhibition of interleukin 10 by rituximab results in down-regulation of bcl-2 and sensitization of B-cell non-Hodgkin's lymphoma to apoptosis. *Clin Cancer Res* 2001; **7**: 709–23.
18 Alas S, Bonavida B, Emmanouilides C. Potentiation of fludarabine cytotoxicity on non-Hodgkin's lymphoma by pentoxifylline and rituximab. *Anticancer Res* 2000; **20**: 2961–6.
19 Di Gaetano N, Xiao Y, Erba E *et al.* Synergism between fludarabine and rituximab revealed in a follicular lymphoma cell line resistant to the cytotoxic activity of either drug alone. *Br J Haematol* 2001; **114**: 800–9.
20 Demidem A, Lam T, Alas S *et al.* Chimeric anti-CD20 (IDEC-C2B8) monoclonal antibody sensitizes a B cell lymphoma cell line to cell killing by cytotoxic drugs. *Cancer Biother Radiopharm* 1997; **12**: 177–86.
21 Czuczman MS, Koryzna A, Mohr A *et al.* Rituximab in combination with

fludarabine chemotherapy in low-grade or follicular lymphoma. *J Clin Oncol* 2005; **23**: 694–704.
22 Ogawa Y, Hotta T, Tobinai K *et al.* Phase I and pharmacokinetic study of oral fludarabine phosphate in relapsed indolent B-cell non-Hodgkin's lymphoma. *Ann Oncol* 2006; **17**: 330–3.
23 Tobinai K, Watanabe T, Ogura M *et al.* Phase II study of oral fludarabine phosphate in relapsed indolent B-cell non-Hodgkin's lymphoma. *J Clin Oncol* 2006; **24**: 174–80.
24 Harris NL, Jaffe ES, Diebold J *et al.* World Health Organization classification of neoplastic diseases of the hematopoietic and lymphoid tissues: Report of the Clinical Advisory Committee Meeting-Airlie House, Virginia, November 1997. *J Clin Oncol* 1999; **17**: 3835–49.
25 Oken MM, Creech RH, Tormey DC *et al.* Toxicity and response criteria of Eastern Cooperative Oncology Group. *Am J Clin Oncol* 1982; **5**: 649–55.
26 Cheson BD, Horning SJ, Coiffier B *et al.* Report of an international workshop to standardize response criteria for non-Hodgkin's lymphomas. *J Clin Oncol* 1999; **17**: 1244–53.
27 Solal-Celigny P, Roy P, Colombat P *et al.* Follicular lymphoma international prognostic index. *Blood* 2004; **104**: 1258–65.
28 Ogura M, Morishima Y, Kobayashi Y *et al.* Durable response but prolonged cytopenia after cladribine treatment in relapsed patients with indolent non-Hodgkin's lymphomas: results of a Japanese phase II study. *Int J Hematol* 2004; **80**: 267–77.
29 McLaughlin P, Grillo-López AJ, Link BK *et al.* Rituximab chimeric anti-CD20 monoclonal antibody therapy for relapsed indolent lymphoma: half of patients respond to a four-dose treatment program. *J Clin Oncol* 1998; **16**: 2825–33.
30 Igarashi T, Kobayashi Y, Ogura M *et al.* Factors affecting toxicity, response and progression-free survival in relapsed patients with indolent B-cell lymphoma and mantle cell lymphoma treated with rituximab: a Japanese phase II study. *Ann Oncol* 2002; **13**: 928–43.
31 Witzig TE, Gordon LI, Cabanillas F *et al.* Randomized controlled trial of yttrium-90-labeled ibritumomab tiuxetan radioimmunotherapy versus rituximab immunotherapy for patients with relapsed or refractory low-grade, follicular, or transformed B-cell non-Hodgkin's lymphoma. *J Clin Oncol* 2002; **20**: 2453–63.
32 Rummel MJ, Al-Batran SE, Kim SZ *et al.* Bendamustine plus rituximab is effective and has a favorable toxicity profile in the treatment of mantle cell and low-grade non-Hodgkin's lymphoma. *J Clin Oncol* 2005; **23**: 3383–9.
33 Robinson KS, Williams ME, van der Jagt RH *et al.* Phase II multicenter study of bendamustine plus rituximab in patients with relapsed indolent B-cell and mantle cell non-Hodgkin's lymphoma. *J Clin Oncol* 2008; **26**: 4473–9.
34 Nitta E, Izutsu K, Sato T *et al.* A high incidence of late-onset neutropenia following rituximab-containing chemotherapy as a primary treatment of CD20-positive B-cell lymphoma: a single-institution study. *Ann Oncol* 2007; **18**: 364–9.

doi: 10.1111/j.1349-7006.2009.01247.x

nature

Vol 459|4 June 2009|doi:10.1038/nature07969

LETTERS

Frequent inactivation of A20 in B-cell lymphomas

Motohiro Kato[1,2], Masashi Sanada[1,5], Itaru Kato[6], Yasuharu Sato[7], Junko Takita[1,2,3], Kengo Takeuchi[8], Akira Niwa[6], Yuyan Chen[1,2], Kumi Nakazaki[1,4,5], Junko Nomoto[9], Yoshitaka Asakura[9], Satsuki Muto[1], Azusa Tamura[1], Mitsuru Iio[1], Yoshiki Akatsuka[11], Yasuhide Hayashi[12], Hiraku Mori[13], Takashi Igarashi[2], Mineo Kurokawa[4], Shigeru Chiba[3], Shigeo Mori[14], Yuichi Ishikawa[8], Koji Okamoto[10], Kensei Tobinai[9], Hitoshi Nakagama[10], Tatsutoshi Nakahata[6], Tadashi Yoshino[7], Yukio Kobayashi[9] & Seishi Ogawa[1,5]

A20 is a negative regulator of the NF-κB pathway and was initially identified as being rapidly induced after tumour-necrosis factor-α stimulation[1]. It has a pivotal role in regulation of the immune response and prevents excessive activation of NF-κB in response to a variety of external stimuli[2–7]; recent genetic studies have disclosed putative associations of polymorphic *A20* (also called *TNFAIP3*) alleles with autoimmune disease risk[8,9]. However, the involvement of A20 in the development of human cancers is unknown. Here we show, using a genome-wide analysis of genetic lesions in 238 B-cell lymphomas, that *A20* is a common genetic target in B-lineage lymphomas. A20 is frequently inactivated by somatic mutations and/or deletions in mucosa-associated tissue lymphoma (18 out of 87; 21.8%) and Hodgkin's lymphoma of nodular sclerosis histology (5 out of 15; 33.3%), and, to a lesser extent, in other B-lineage lymphomas. When re-expressed in a lymphoma-derived cell line with no functional *A20* alleles, wild-type A20, but not mutant A20, resulted in suppression of cell growth and induction of apoptosis, accompanied by downregulation of NF-κB activation. The A20-deficient cells stably generated tumours in immunodeficient mice, whereas the tumorigenicity was effectively suppressed by re-expression of A20. In A20-deficient cells, suppression of both cell growth and NF-κB activity due to re-expression of A20 depended, at least partly, on cell-surface-receptor signalling, including the tumour-necrosis factor receptor. Considering the physiological function of A20 in the negative modulation of NF-κB activation induced by multiple upstream stimuli, our findings indicate that uncontrolled signalling of NF-κB caused by loss of A20 function is involved in the pathogenesis of subsets of B-lineage lymphomas.

Malignant lymphomas of B-cell lineages are mature lymphoid neoplasms that arise from various lymphoid tissues[10,11]. To obtain a comprehensive registry of genetic lesions in B-lineage lymphomas, we performed a single nucleotide polymorphism (SNP) array analysis of 238 primary B-cell lymphoma specimens of different histologies, including 64 samples of diffuse large B-cell lymphomas (DLBCLs), 52 follicular lymphomas, 35 mantle cell lymphomas (MCLs), and 87 mucosa-associated tissue (MALT) lymphomas (Supplementary Table 1). Three Hodgkin's-lymphoma-derived cell lines were also analysed. Interrogating more than 250,000 SNP sites, this platform permitted the identification of copy number changes at an average resolution of less than 12 kilobases (kb). The use of large numbers of SNP-specific probes is a unique feature of this platform, and combined with the CNAG/AsCNAR software, enabled accurate determination of 'allele-specific' copy numbers, and thus allowed for sensitive detection of loss of heterozygosity (LOH) even without apparent copy-number reduction, in the presence of up to 70–80% normal cell contamination[12,13].

Lymphoma genomes underwent a wide range of genetic changes, including numerical chromosomal abnormalities and segmental gains and losses of chromosomal material (Supplementary Fig. 1), as well as copy-number-neutral LOH, or uniparental disomy (Supplementary Fig. 2). Each histology type had a unique genomic signature, indicating a distinctive underlying molecular pathogenesis for different histology types (Fig. 1a and Supplementary Fig. 3). On the basis of the genomic signatures, the initial pathological diagnosis of MCL was re-evaluated and corrected to DLBCL in two cases. Although most copy number changes involved large chromosomal segments, a number of regions showed focal gains and deletions, accelerating identification of their candidate gene targets. After excluding known copy number variations, we identified 46 loci showing focal gains (19 loci) or deletions (27 loci) (Supplementary Tables 2 and 3 and Supplementary Fig. 4).

Genetic lesions on the NF-κB pathway were common in B-cell lymphomas and found in approximately 40% of the cases (Supplementary Table 1), underpinning the importance of aberrant NF-κB activation in lymphomagenesis[11,14] in a genome-wide fashion. They included focal gain/amplification at the *REL* locus (16.4%) (Fig. 1b) and *TRAF6* locus (5.9%), as well as focal deletions at the *PTEN* locus (5.5%) (Supplementary Figs 1 and 4). However, the most striking finding was the common deletion at 6q23.3 involving a 143-kb segment. It exclusively contained the *A20* gene (also called *TNFAIP3*), a negative regulator of NF-κB activation[3–7,15] (Fig. 1b), which was previously reported as a candidate target of 6q23 deletions in ocular lymphoma[16]. LOH involving the *A20* locus was found in 50 cases, of which 12 showed homozygous deletions as determined by the loss of both alleles in an allele-specific copy number analysis (Fig. 1b, Table 1 and Supplementary Table 4). On the basis of this finding, we searched for possible tumour-specific mutations of *A20* by genomic DNA sequencing of entire coding exons of the gene in the same series of lymphoma samples (Supplementary Fig. 5). Because two out of the three Hodgkin's-lymphoma-derived cell lines had biallelic *A20* deletions/mutations (Supplementary Fig. 6), 24 primary samples from Hodgkin's lymphoma were also analysed for mutations, where

[1]Cancer Genomics Project, Department of [2]Pediatrics, [3]Cell Therapy and Transplantation Medicine, and [4]Hematology and Oncology, Graduate School of Medicine, University of Tokyo, 7-3-1 Hongo, Bunkyo-ku, Tokyo 113-8655, Japan. [5]Core Research for Evolutional Science and Technology, Japan Science and Technology Agency, 4-1-8, Honcho, Kawaguchi-shi, Saitama 332-0012, Japan. [6]Department of Pediatrics, Graduate School of Medicine, Kyoto University, 54 Kawahara-cho, Shogoin, Sakyo-ku, Kyoto 606-8507, Japan. [7]Department of Pathology, Okayama University Graduate School of Medicine, Dentistry and Pharmaceutical Sciences, 2-5-1 Shikata-cho, Kita-ku, Okayama 700-8558, Japan. [8]Division of Pathology, The Cancer Institute of Japanese Foundation for Cancer Research, Japan, 3-10-6 Ariake, Koto-ku, Tokyo 135-8550, Japan. [9]Hematology Division, Hospital, and [10]Early Oncogenesis Research Project, Research Institute, National Cancer Center, 5-1-1 Tsukiji, Chuo-ku, Tokyo 104-0045, Japan. [11]Division of Immunology, Aichi Cancer Center Research Institute, 1-1 Kanokoden, Chikusa-ku, Nagoya 464-8681, Japan. [12]Gunma Children's Medical Center, 779 Shimohakoda, Hokkitsu-machi, Shibukawa 377-8577, Japan. [13]Division of Hematology, Internal Medicine, Showa University Fujigaoka Hospital, 1-30, Fujigaoka, Aoba-ku, Yokohama-shi, Kanagawa 227-8501, Japan. [14]Department of Pathology, Teikyo University School of Medicine, 2-11-1 Kaga, Itabashi-ku, Tokyo 173-8605, Japan.

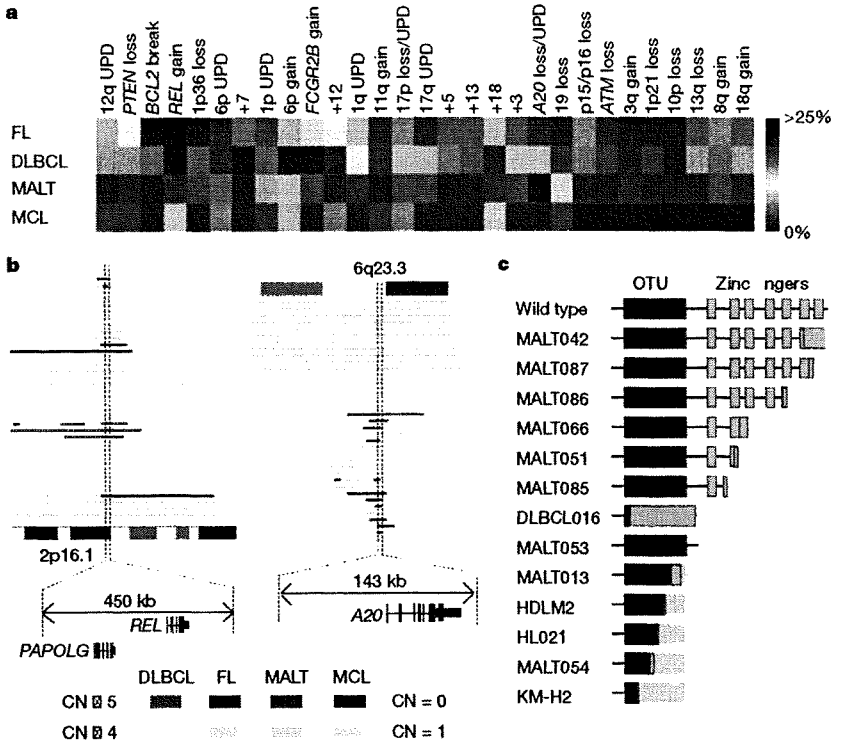

Figure 1 | Genomic signatures of different B-cell lymphomas and common genetic lesions at 2p16-15 and 6q23.3 involving NF-κB pathway genes. **a**, Twenty-nine genetic lesions were found in more than 10% in at least one histology and used for clustering four distinct histology types of B-lineage lymphomas. The frequency of each genetic lesion in each histology type is colour-coded. FL, follicular lymphoma; UPD, uniparental disomy. **b**, Recurrent genetic changes are depicted based on CNAG output of the SNP array analysis of 238 B-lineage lymphoma samples, which include gains at the *REL* locus on 2p16-15 (left panel) and the *A20* locus on 6q23.3 (right panel). Regions showing copy number gain or loss are indicated by horizontal lines. Four histology types are indicated by different colours, where high-grade amplifications and homozygous deletions are shown by darker shades to discriminate from simple gains (copy number ≤4) and losses (copy number = 1) (lighter shades). **c**, Point mutations and small nucleotide insertions and deletions in the *A20* (*TNFAIP3*) gene caused premature truncation of A20 in most cases. Altered amino acids caused by frame shifts are indicated by green bars.

genomic DNA was extracted from 150 microdissected CD30-positive tumour cells (Reed–Sternberg cells) for each sample. *A20* mutations were found in 18 out of 265 lymphoma samples (6.8%) (Table 1), among which 13 mutations, including nonsense mutations (3 cases), frame-shift insertions/deletions (9 cases), and a splicing donor site mutation (1 case) were thought to result in premature termination of translation (Fig. 1c). Four missense mutations and one intronic mutation were identified in five microdissected Hodgkin's lymphoma samples. They were not found in the surrounding normal tissues, and thus, were considered as tumour-specific somatic changes.

In total, biallelic *A20* lesions were found in 31 out of 265 lymphoma samples including 3 Hodgkin's lymphoma cell lines. Quantitative analysis of SNP array data suggested that these *A20* lesions were present in the major tumour fraction within the samples (Supplementary Fig. 7). Inactivation of *A20* was most frequent in MALT lymphoma (18 out of 87) and Hodgkin's lymphoma (7 out of 27), although it was also found in DLBCL (5 out of 64) and follicular lymphoma (1 out of 52) at lower frequencies. In MALT lymphoma, biallelic *A20* lesions were confirmed in 18 out of 24 cases (75.0%) with LOH involving the 6q23.3 segment (Supplementary Fig. 8). Considering the limitation in detecting very small homozygous deletions, *A20* was thought to be the target of 6q23 LOH in MALT lymphoma. On the other hand, the 6q23 LOHs in other histology types tended to be extended into more centromeric regions and less frequently accompanied biallelic *A20* lesions (Supplementary Fig. 8 and Supplementary Table 4), indicating that they might be more heterogeneous with regard to their gene targets. We were unable to analyse Hodgkin's lymphoma samples using SNP arrays owing to insufficient genomic DNA obtained from microdissected samples, and were likely to underestimate the frequency of *A20* inactivation in Hodgkin's lymphoma because we might fail to detect a substantial proportion of cases with homozygous deletions, which explained 50% (12 out of 24) of *A20* inactivation in other histology types. *A20* mutations in Hodgkin's lymphoma were exclusively found in nodular sclerosis classical Hodgkin's lymphoma (5 out of 15) but not in other histology types (0 out of 9), although the possible association requires further confirmation in additional cases.

A20 is a key regulator of NF-κB signalling, negatively modulating NF-κB activation through a wide variety of cell surface receptors and viral proteins, including tumour-necrosis factor (TNF) receptors, toll-like receptors, CD40, as well as Epstein–Barr-virus-associated LMP1 protein[2,5,17,18]. To investigate the role of A20 inactivation in lymphomagenesis, we re-expressed wild-type A20 under a *Tet*-inducible promoter in a lymphoma-derived cell line (KM-H2) that had no functional *A20* alleles (Supplementary Fig. 6), and examined the effect of A20 re-expression on cell proliferation, survival and downstream NF-κB signalling pathways. As shown in Fig. 2a–c and Supplementary Fig. 9, re-expression of wild-type A20 resulted in the suppression of cell proliferation and enhanced apoptosis, and in the concomitant accumulation of IκBβ and IκBε, and downregulation of NF-κB activity. In contrast, re-expression of two lymphoma-derived A20 mutants, $A20^{532Stop}$ or $A20^{750Stop}$, failed to show growth suppression, induction of apoptosis, accumulation of IκBβ and IκBε or downregulation of

Table 1 | Inactivation of A20 in B-lineage lymphomas

Histology	Tissue	Sample	Allele	Uniparental disomy	Exon	Mutation	Biallelic inactivation
DLBCL							5 out of 64 (7.8%)
	Lymph node	DLBCL008	−/−	No	–	–	
	Lymph node	DLBCL016	+/−	No	Ex2	329insA	
	Lymph node	DLBCL022	−/−	No	–	–	
	Lymph node	DLBCL028	−/−	Yes	–	–	
	Lymph node	MCL008*	−/−	Yes	–	–	
Follicular lymphoma							1 out of 52 (1.9%)
	Lymph node	FL024	−/−	No	–	–	
MCL							0 out of 35 (0%)
MALT							18 out of 87 (21.8%)
Stomach							3 out of 23 (13.0%)
	Gastric mucosa	MALT013	+/+	Yes	Ex5	705insG	
	Gastric mucosa	MALT014	+/+	Yes	Ex3	Ex3 donor site>A	
	Gastric mucosa	MALT036	+/−	No	Ex7	delintron6–Ex7†	
Eye							13 out of 43 (30.2%)
	Ocular adnexa	MALT008	−/−	No	–	–	
	Ocular adnexa	MALT017	−/−	No	–	–	
	Ocular adnexa	MALT051	+/−	No	Ex7	1943delTG	
	Ocular adnexa	MALT053	+/+	Yes	Ex6	1016G>A(stop)	
	Ocular adnexa	MALT054	+/−	No	Ex3	502delTC	
	Ocular adnexa	MALT055	−/−	No	–	–	
	Ocular adnexa	MALT066	+/−	No	Ex7	1581insA	
	Ocular adnexa	MALT067	−/−	No	–	–	
	Ocular adnexa	MALT082	−/−	Yes	–	–	
	Ocular adnexa	MALT084	−/−	Yes	–	–	
	Ocular adnexa	MALT085	+/+	Yes	Ex7	1435insG	
	Ocular adnexa	MALT086	+/+	Yes	Ex6	878C>T(stop)	
	Ocular adnexa	MALT087	+/+	Yes	Ex9	2304delGG	
Lung							2 out of 12 (16.7%)
	Lung	MALT042	−/−	No	–	–	
	Lung	MALT047	+/+	Yes	Ex9	2281insT	
Other‡							0 out of 9 (0%)
Hodgkin's lymphoma							7 out of 27 (26.0%)
NSHL	Lymph node	HL10	ND	ND	Ex7	1777G>A(V571I)	
NSHL	Lymph node	HL12	ND	ND	Ex7	1156A>G(R364G)	
NSHL	Lymph node	HL21	ND	ND	Ex4	569G>A(stop)	
NSHL	Lymph node	HL24	ND	ND	Ex3	1487C>A(T474N)	
NSHL	Lymph node	HL23	ND	ND	–	Intron 3§	
	Cell line	KM-H2	−/−	No	–		
	Cell line	HDLM2	+/−	No	Ex4	616ins29bp‖	
Total							31 out of 265 (11.7%)

DLBCL, diffuse large B-cell lymphoma; MALT, MALT lymphoma; MCL, mantle cell lymphoma; ND, not determined because SNP array analysis was not performed; NSHL, nodular sclerosis classical Hodgkin's lymphoma.
* Diagnosis was changed based on the genomic data, which was confirmed by re-examination of pathology.
† Deletion including the boundary of intron 6 and exon 7 (see also Supplementary Fig. 5b).
‡ Including 1 parotid gland, 1 salivary gland, 2 colon and 5 thyroid cases.
§ Insertion of CTC at −19 bases from the beginning of exon 3.
‖ Insertion of TGGCTTCCACAGACACACCCATGGCCCGA.

NF-κB activity (Fig. 2a–c), indicating that these were actually loss-of-function mutations. To investigate the role of A20 inactivation in lymphomagenesis *in vivo*, *A20*- and mock-transduced KM-H2 cells were transplanted in NOD/SCID/γ_c^{null} (NOG) mice[19], and their tumour formation status was examined for 5 weeks with or without induction of wild-type A20 by tetracycline administration. As shown in Fig. 2d, mock-transduced cells developed tumours at the injected sites, whereas the *Tet*-inducible *A20*-transduced cells generated tumours only in the absence of A20 induction (Supplementary Table 5), further supporting the tumour suppressor role of A20 in lymphoma development.

Given the mode of negative regulation of NF-κB signalling, we next investigated the origins of NF-κB activity that was deregulated by A20 loss in KM-H2 cells. The conditioned medium prepared from a 48-h serum-free KM-H2 culture had increased NF-κB upregulatory activity compared with fresh serum-free medium, which was inhibited by re-expression of A20 (Fig. 3a). KM-H2 cells secreted two known ligands for TNF receptor—TNF-α and lymphotoxin-α (Supplementary Fig. 10)[20]—and adding neutralizing antibodies against these cytokines into cultures significantly suppressed their cell growth and NF-κB activity without affecting the levels of their overall suppression after A20 induction (Fig. 3b, d). In addition, recombinant TNF-α and/or lymphotoxin-α added to fresh serum-free medium promoted cell growth and NF-κB activation in KM-H2 culture, which were again suppressed by re-expression of A20 (Fig. 3c, e). Although our data in Fig. 3 also show the presence of factors other than TNF-α and lymphotoxin-α in the KM-H2-conditioned medium—as well as some intrinsic pathways in the cell (Fig. 3a)—that were responsible for the A20-dependent NF-κB activation, these results indicate that both cell growth and NF-κB activity that were upregulated by A20 inactivation depend at least partly on the upstream stimuli that evoked the NF-κB-activating signals.

Aberrant activation of the NF-κB pathway is a hallmark of several subtypes of B-lineage lymphomas, including Hodgkin's lymphoma, MALT lymphoma, and a subset of DLBCL, as well as other lymphoid neoplasms[11,14], where a number of genetic alterations of NF-κB signalling pathway genes[21–25], as well as some viral proteins[26,27], have been implicated in the aberrant activation of the NF-κB pathway[14]. Thus, frequent inactivation of A20 in Hodgkin's lymphoma and MALT and other lymphomas provides a novel insight into the molecular pathogenesis of these subtypes of B-lineage lymphomas through deregulated NF-κB activation. Because A20 provides a

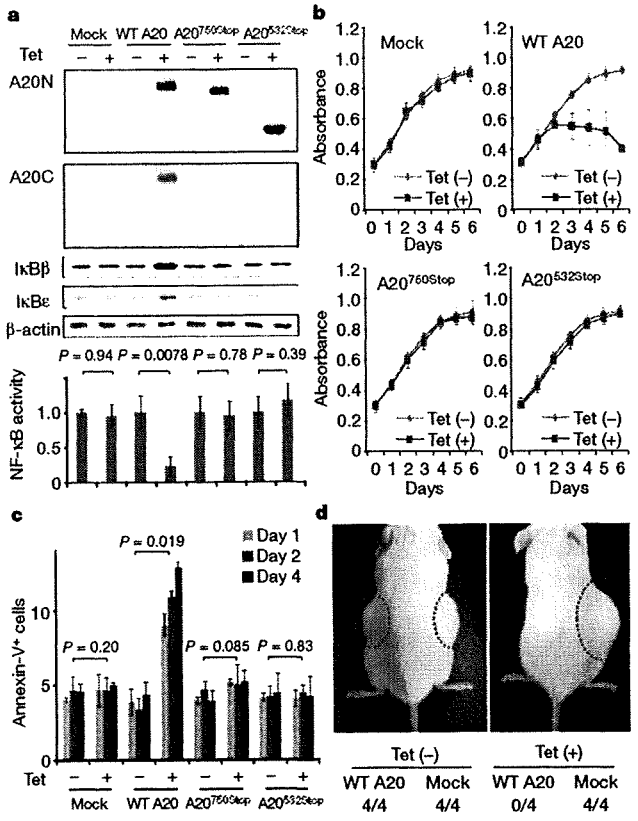

Figure 2 | Effects of wild-type and mutant A20 re-expressed in a lymphoma cell line that lacks the normal *A20* gene. **a**, Western blot analyses of wild-type (WT) and mutant ($A20^{532Stop}$ and $A20^{750Stop}$) A20, as well as IκBβ and IκBε, in KM-H2 cells, in the presence or absence of tetracycline treatment (top panels). A20N and A20C are polyclonal antisera raised against N-terminal and C-terminal A20 peptides, respectively. β-actin blots are provided as a control. NF-κB activities are expressed as mean absorbance ± s.d. ($n = 6$) in luciferase assays (bottom panel). **b**, Proliferation of KM-H2 cells stably transduced with plasmids for mock and *Tet*-inducible wild-type A20, $A20^{532Stop}$ and $A20^{750Stop}$ was measured using a cell counting kit in the presence (red lines) or absence (blue lines) of tetracycline. Mean absorbance ± s.d. ($n = 5$) is plotted. **c**, The fractions of Annexin-V-positive KM-H2 cells transduced with various *Tet*-inducible A20 constructs were measured by flow cytometry after tetracycline treatment and the mean values (±s.d., $n = 3$) are plotted. **d**, *In vivo* tumorigenicity was assayed by inoculating 7×10^6 KM-H2 cells transduced with mock or *Tet*-inducible wild-type A20 in NOG mice, with (right panel) or without (left panel) tetracycline administration.

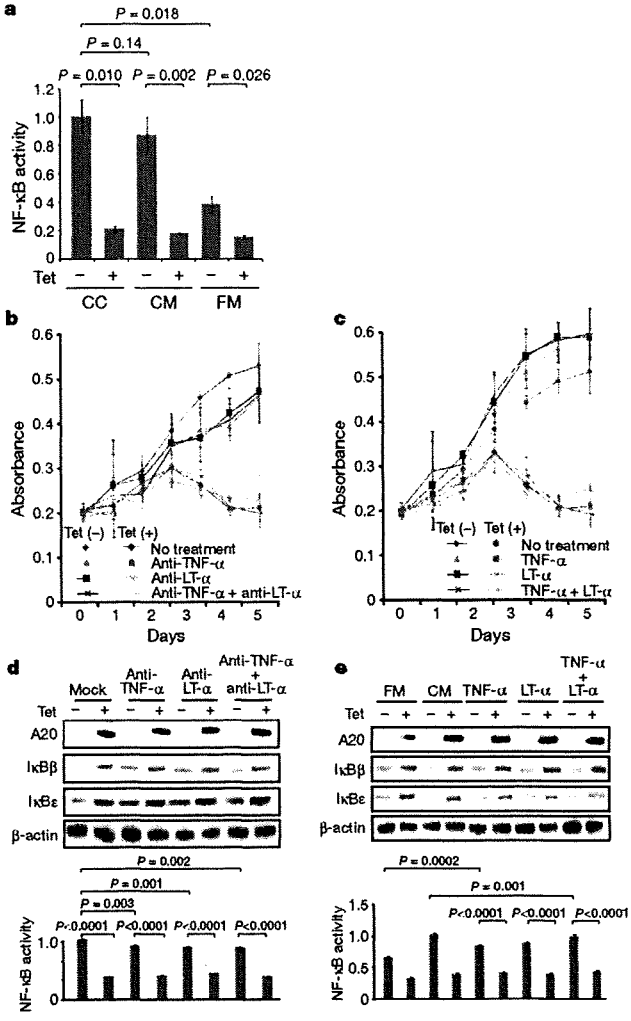

Figure 3 | Tumour suppressor role of A20 under external stimuli. **a**, NF-κB activity in KM-H2 cells was measured 30 min after cells were inoculated into fresh medium (FM) or KM-H2-conditioned medium (CM) obtained from the 48-h culture of KM-H2, and was compared with the activity after 48 h continuous culture of KM-H2 (CC). A20 was induced 12 h before inoculation in Tet (+) groups. **b**, **c**, Effects of neutralizing antibodies against TNF-α and lymphotoxin-α (LTα) (**b**) and of recombinant TNF-α and LT-α added to the culture (**c**) on cell growth were evaluated in the presence (Tet (+)) or absence (Tet (−)) of A20 induction. Cell numbers were measured using a cell counting kit and are plotted as their mean absorbance ± s.d. ($n = 6$). **d**, **e**, Effects of the neutralizing antibodies (**d**) and the recombinant cytokines added to the culture (**e**) on NF-κB activities and the levels of IκBβ and IκBε after 48 h culture with (Tet (+)) or without (Tet (−)) tetracycline treatment. NF-κB activities are expressed as mean absorbance ± s.d. ($n = 6$) in luciferase assays.

negative feedback mechanism in the regulation of NF-κB signalling pathways upon a variety of stimuli, aberrant activation of NF-κB will be a logical consequence of A20 inactivation. However, there is also the possibility that the aberrant NF-κB activity of A20-inactivated lymphoma cells is derived from upstream stimuli, which may be from the cellular environment. In this context, it is intriguing that MALT lymphoma usually arises at the site of chronic inflammation caused by infection or autoimmune disorders and may show spontaneous regression after eradication of infectious organisms[28]; furthermore, Hodgkin's lymphoma frequently shows deregulated cytokine production from Reed–Sternberg cells and/or surrounding reactive cells[29]. Detailed characterization of the NF-κB pathway regulated by A20 in both normal and neoplastic B lymphocytes will promote our understanding of the precise roles of A20 inactivation in the pathogenesis of these lymphoma types. Our finding underscores the importance of genome-wide approaches in the identification of genetic targets in human cancers.

METHODS SUMMARY

Genomic DNA from 238 patients with non-Hodgkin's lymphoma and three Hodgkin's-lymphoma-derived cell lines was analysed using GeneChip SNP genotyping microarrays (Affymetrix). This study was approved by the ethics boards of the University of Tokyo, National Cancer Institute Hospital, Okayama University, and the Cancer Institute of the Japanese Foundation of Cancer Research. After appropriate normalization of mean array intensities, signal ratios between tumours and anonymous normal references were calculated in an allele-specific manner, and allele-specific copy numbers were inferred from the observed signal ratios based on the hidden Markov model using CNAG/AsCNAR software (http://www.genome.umin.jp). *A20* mutations were examined by directly sequencing genomic DNA using a set of primers (Supplementary Table 6). Full-length cDNAs of wild-type and mutant *A20* were introduced into a

lentivirus vector, pLenti4/TO/V5-DEST (Invitrogen), with a *Tet*-inducible promoter. Viral stocks were prepared by transfecting the vector plasmids into 293FT cells (Invitrogen) using the calcium phosphate method and then infected to the KM-H2 cell line. Proliferation of KM-H2 cells was measured using a Cell Counting Kit (Dojindo). Western blot analyses and luciferase assays were performed as previously described. NF-κB activity was measured by luciferase assays in KM-H2 cells stably transduced with a reporter plasmid having an NF-κB response element, pGL4.32 (Promega). Apoptosis of KM-H2 upon A20 induction was evaluated by counting Annexin-V-positive cells by flow cytometry. For *in vivo* tumorigenicity assays, 7×10^6 KM-H2 cells were transduced with the *Tet*-inducible *A20* gene and those with a mock vector were inoculated on the contralateral sides in eight NOG mice[19] and examined for their tumour formation with ($n = 4$) or without ($n = 4$) tetracycline administration. Full copy number data of the 238 lymphoma samples will be accessible from the Gene Expression Omnibus (GEO, http://ncbi.nlm.nih.gov/geo/) with the accession number GSE12906.

Full Methods and any associated references are available in the online version of the paper at www.nature.com/nature.

Received 17 September 2008; accepted 3 March 2009.
Published online 3 May 2009.

1. Dixit, V. M. *et al.* Tumor necrosis factor-α induction of novel gene products in human endothelial cells including a macrophage-specific chemotaxin. *J. Biol. Chem.* **265**, 2973–2978 (1990).
2. Song, H. Y., Rothe, M. & Goeddel, D. V. The tumor necrosis factor-inducible zinc finger protein A20 interacts with TRAF1/TRAF2 and inhibits NF-κB activation. *Proc. Natl Acad. Sci. USA* **93**, 6721–6725 (1996).
3. Lee, E. G. *et al.* Failure to regulate TNF-induced NF-κB and cell death responses in A20-deficient mice. *Science* **289**, 2350–2354 (2000).
4. Boone, D. L. *et al.* The ubiquitin-modifying enzyme A20 is required for termination of Toll-like receptor responses. *Nature Immunol.* **5**, 1052–1060 (2004).
5. Wang, Y. Y., Li, L., Han, K. J., Zhai, Z. & Shu, H. B. A20 is a potent inhibitor of TLR3- and Sendai virus-induced activation of NF-κB and ISRE and IFN-β promoter. *FEBS Lett.* **576**, 86–90 (2004).
6. Wertz, I. E. *et al.* De-ubiquitination and ubiquitin ligase domains of A20 downregulate NF-κB signalling. *Nature* **430**, 694–699 (2004).
7. Heyninck, K. & Beyaert, R. A20 inhibits NF-κB activation by dual ubiquitin-editing functions. *Trends Biochem. Sci.* **30**, 1–4 (2005).
8. Graham, R. R. *et al.* Genetic variants near *TNFAIP3* on 6q23 are associated with systemic lupus erythematosus. *Nature Genet.* **40**, 1059–1061 (2008).
9. Musone, S. L. *et al.* Multiple polymorphisms in the *TNFAIP3* region are independently associated with systemic lupus erythematosus. *Nature Genet.* **40**, 1062–1064 (2008).
10. Jaffe, E. S., Harris, N. L., Stein, H. & Vardiman, J. W. *World Health Organization Classification of Tumours. Pathology and Genetics of Tumours of Hematopoietic and Lymphoid Tissues* (IARC Press, 2001).
11. Klein, U. & Dalla-Favera, R. Germinal centres: role in B-cell physiology and malignancy. *Nature Rev. Immunol.* **8**, 22–33 (2008).
12. Nannya, Y. *et al.* A robust algorithm for copy number detection using high-density oligonucleotide single nucleotide polymorphism genotyping arrays. *Cancer Res.* **65**, 6071–6079 (2005).
13. Yamamoto, G. *et al.* Highly sensitive method for genomewide detection of allelic composition in nonpaired, primary tumor specimens by use of affymetrix single-nucleotide-polymorphism genotyping microarrays. *Am. J. Hum. Genet.* **81**, 114–126 (2007).
14. Jost, P. J. & Ruland, J. Aberrant NF-κB signaling in lymphoma: mechanisms, consequences, and therapeutic implications. *Blood* **109**, 2700–2707 (2007).
15. Durkop, H., Hirsch, B., Hahn, C., Foss, H. D. & Stein, H. Differential expression and function of A20 and TRAF1 in Hodgkin lymphoma and anaplastic large cell lymphoma and their induction by CD30 stimulation. *J. Pathol.* **200**, 229–239 (2003).
16. Honma, K. *et al. TNFAIP3* is the target gene of chromosome band 6q23.3-q24.1 loss in ocular adnexal marginal zone B cell lymphoma. *Genes Chromosom. Cancer* **47**, 1–7 (2008).
17. Sarma, V. *et al.* Activation of the B-cell surface receptor CD40 induces A20, a novel zinc finger protein that inhibits apoptosis. *J. Biol. Chem.* **270**, 12343–12346 (1995).
18. Fries, K. L., Miller, W. E. & Raab-Traub, N. The A20 protein interacts with the Epstein-Barr virus latent membrane protein 1 (LMP1) and alters the LMP1/TRAF1/TRADD complex. *Virology* **264**, 159–166 (1999).
19. Hiramatsu, H. *et al.* Complete reconstitution of human lymphocytes from cord blood $CD34^+$ cells using the NOD/SCID/γ^{null} mice model. *Blood* **102**, 873–880 (2003).
20. Hsu, P. L. & Hsu, S. M. Production of tumor necrosis factor-α and lymphotoxin by cells of Hodgkin's neoplastic cell lines HDLM-1 and KM-H2. *Am. J. Pathol.* **135**, 735–745 (1989).
21. Dierlamm, J. *et al.* The apoptosis inhibitor gene *API2* and a novel 18q gene, *MLT*, are recurrently rearranged in the t(11;18)(q21;q21) associated with mucosa-associated lymphoid tissue lymphomas. *Blood* **93**, 3601–3609 (1999).
22. Willis, T. G. *et al.* Bcl10 is involved in t(1;14)(p22;q32) of MALT B cell lymphoma and mutated in multiple tumor types. *Cell* **96**, 35–45 (1999).
23. Joos, S. *et al.* Classical Hodgkin lymphoma is characterized by recurrent copy number gains of the short arm of chromosome 2. *Blood* **99**, 1381–1387 (2002).
24. Martin-Subero, J. I. *et al.* Recurrent involvement of the *REL* and *BCL11A* loci in classical Hodgkin lymphoma. *Blood* **99**, 1474–1477 (2002).
25. Lenz, G. *et al.* Oncogenic *CARD11* mutations in human diffuse large B cell lymphoma. *Science* **319**, 1676–1679 (2008).
26. Deacon, E. M. *et al.* Epstein-Barr virus and Hodgkin's disease: transcriptional analysis of virus latency in the malignant cells. *J. Exp. Med.* **177**, 339–349 (1993).
27. Yin, M. J. *et al.* HTLV-I Tax protein binds to MEKK1 to stimulate IκB kinase activity and NF-κB activation. *Cell* **93**, 875–884 (1998).
28. Isaacson, P. G. & Du, M. Q. MALT lymphoma: from morphology to molecules. *Nature Rev. Cancer* **4**, 644–653 (2004).
29. Skinnider, B. F. & Mak, T. W. The role of cytokines in classical Hodgkin lymphoma. *Blood* **99**, 4283–4297 (2002).

Supplementary Information is linked to the online version of the paper at www.nature.com/nature.

Acknowledgements This work was supported by the Core Research for Evolutional Science and Technology, Japan Science and Technology Agency, by the 21st century centre of excellence program 'Study on diseases caused by environment/genome interactions', and by Grant-in-Aids from the Ministry of Education, Culture, Sports, Science and Technology of Japan and from the Ministry of Health, Labor and Welfare of Japan for the 3rd-term Comprehensive 10-year Strategy for Cancer Control. We also thank Y. Ogino, E. Matsui and M. Matsumura for their technical assistance.

Author Contributions M.Ka., K.N. and M.S. performed microarray experiments and subsequent data analyses. M.Ka., Y.C., K.Ta., J.T., J.N., M.I., A.T. and Y.K. performed mutation analysis of *A20*. M.Ka., S.Mu., M.S., Y.C. and Y.Ak. conducted functional assays of mutant A20. Y.S., K.Ta., Y.As., H.M., M.Ku., S.Mo., S.C., Y.K., K.To. and Y.I. prepared tumour specimens. I.K., K.O., A.N., H.N. and T.N. conducted *in vivo* tumorigenicity experiments in NOG/SCID mice. T.I., Y.H., T.Y., Y.K. and S.O. designed overall studies, and S.O. wrote the manuscript. All authors discussed the results and commented on the manuscript.

Author Information The copy number data as well as the raw microarray data will be accessible from the GEO (http://ncbi.nlm.nih.gov/geo/) with the accession number GSE12906. Reprints and permissions information is available at www.nature.com/reprints. Correspondence and requests for materials should be addressed to S.O. (sogawa-tky@umin.ac.jp) or Y.K. (ykkobaya@ncc.go.jp).

METHODS

Specimens. Primary tumour specimens were obtained from patients who were diagnosed with DLBCL, follicular lymphoma, MCL, MALT lymphoma, or classical Hodgkin's lymphoma. In total, 238 primary lymphoma specimens listed in Supplementary Table 1 were subjected to SNP array analysis. Three Hodgkin's-lymphoma-derived cell lines (KM-H2, HDLM2, L540) were obtained from Hayashibara Biochemical Laboratories, Inc., Fujisaki Cell Center and were also analysed by SNP array analysis.

Microarray analysis. High-molecular-mass DNA was isolated from tumour specimens and subjected to SNP array analysis using GeneChip Mapping 50K and/or 250K arrays (Affymetrix). The scanned array images were processed with Gene Chip Operation software (GCOS), followed by SNP calls using GTYPE. Genome-wide copy number measurements and LOH detection were performed using CNAG/AsCNAR software[12,13].

Mutation analysis. Mutations in the *A20* gene were examined in 265 samples of B-lineage lymphoma, including 62 DLBCLs, 52 follicular lymphomas, 87 MALTs, 37 MCLs and 3 Hodgkin's-lymphoma-derived cell lines and 24 primary Hodgkin's lymphoma samples, by direct sequencing using an ABI PRISM 3130xl Genetic Analyser (Applied Biosystems). To analyse primary Hodgkin's lymphoma samples in which CD30-positive tumour cells (Reed–Sternberg cells) account for only a fraction of the specimen, 150 Reed–Sternberg cells were collected for each 10 μm slice of a formalin-fixed block immunostained for CD30 by laser-capture microdissection (ASLMD6000, Leica), followed by genomic DNA extraction using QIAamp DNA Micro kit (Qiagen). The primer sets used in this study are listed in Supplementary Table 6.

Functional analysis of wild-type and mutant A20. Full-length cDNA for wild-type *A20* was isolated from total RNA extracted from an acute myeloid leukaemia-derived cell line, CTS, and subcloned into a lentivirus vector (pLenti4/TO/V5-DEST, Invitrogen). cDNAs for mutant A20 were generated by PCR amplification using mutagenic primers (Supplementary Table 6), and introduced into the same lentivirus vector. Forty-eight hours after transfection of each plasmid into 293FT cells using the calcium phosphate method, lentivirus stocks were obtained from ultrafiltration using Amicon Ultra (Millipore), and used to infect KM-H2 cells to generate stable transfectants of mock, wild-type and mutant A20. Each KM-H2 derivative cell line was further transduced stably with a reporter plasmid (pGL4.32, Promega) containing a luciferase gene under an NF-κB-responsive element by electroporation using Nucleofector reagents (Amaxa).

Assays for cell proliferation and NF-κB activity. Proliferation of the KM-H2 derivative cell lines was assayed in triplicate using a Cell Counting Kit (Dojindo). The mean absorption of five independent assays was plotted with s.d. for each derivative line. Two independent KM-H2-derived cell lines were used for each experiment. The NF-κB activity in KM-H2 derivatives for A20 mutants was evaluated by luciferase assays using a PiccaGene Luciferase Assay Kit (TOYO B-Net Co.). Each assay was performed in triplicate and the mean absorption of five independent experiments was plotted with s.d.

Western blot analyses. Polyclonal anti-sera against N-terminal (anti-A20N) and C-terminal (anti-A20C) A20 peptides were generated by immunizing rabbits with these peptides (LSNMRKAVKIRERTPEDIC for anti-A20N and CFQFKQMYG for anti-A20C, respectively). Total cell lysates from KM-H2 cells were separated on 7.5% polyacrylamide gel and subjected to western blot analysis using antibodies to A20 (anti-A20N and anti-A20C), IκBα (sc-847), IκBβ (sc-945), IκBγ (sc-7155) and actin (sc-8432) (Santa Cruz Biotechnology).

Functional analyses of wild-type and mutant A20. Each KM-H2 derivative cell line stably transduced with various *Tet*-inducible A20 constructs was cultured in serum-free medium in the presence or absence of A20 induction using 1 μg ml^{-1} of tetracycline, and cell number was counted every day. 1×10^6 cells of each KM-H2 derivative cell line were analysed for their intracellular levels of IκBβ and IκBε and for NF-κB activities by western blot analyses and luciferase assays, respectively, 12 h after the beginning of cell culture. Effects of human recombinant TNF-α and lymphotoxin-α (210-TA and 211-TB, respectively, R&D Systems) on the NF-κB pathway and cell proliferation were evaluated by adding both cytokines into 10 ml of serum-free cell culture at a concentration of 200 pg ml^{-1}. For cell proliferation assays, culture medium was half replaced every 12 h to minimize the side-effects of autocrine cytokines. Intracellular levels of IκBβ, IκBε and NF-κB were examined 12 h after the beginning of the cell culture. To evaluate the effect of neutralizing TNF-α and lymphotoxin-α, 1×10^6 of KM-H2 cells transduced with both *Tet*-inducible A20 and the NF-κB-luciferase reporter were pre-cultured in serum-free media for 36 h, and thereafter neutralizing antibodies against TNF-α (MAB210, R&D Systems) and/or lymphotoxin-α (AF-211-NA, R&D Systems) were added to the media at a concentration of 200 pg ml^{-1}. After the extended culture during 12 h with or without 1 μg ml^{-1} tetracycline, the intracellular levels of IκBβ and IκBε and NF-κB activities were examined by western blot analysis and luciferase assays, respectively. To examine the effects of A20 re-expression on apoptosis, 1×10^6 KM-H2 cells were cultured for 4 days in 10 ml medium with or without *Tet* induction. After staining with phycoerythrin-conjugated anti-Annexin-V (ID556422, Becton Dickinson), Annexin-V-positive cells were counted by flow cytometry at the indicated times.

***In vivo* tumorigenicity assays.** KM-H2 cells transduced with a mock or *Tet*-inducible wild-type *A20* gene were inoculated into NOG mice and their tumorigenicity was examined for 5 weeks with or without tetracycline administration. Injections of 7×10^6 cells of each KM-H2 cell line were administered to two opposite sites in four mice. Tetracycline was administered in drinking water at a concentration of 200 μg ml^{-1}.

ELISA. Concentrations of TNF-α, lymphotoxin-α, IL-1, IL-2, IL-4, IL-6, IL-12, IL-18 and TGF-β in the culture medium were measured after 48 h using ELISA. For those cytokines detectable after 48-h culture (TNFα, LTα, and IL-6), their time course was examined further using the Quantikine ELISA kit (R&D Systems).

Statistical analysis. Significance of the difference in NF-κB activity between two given groups was evaluated using a paired *t*-test, in which the data from each independent luciferase assay were paired to calculate test statistics. To evaluate the effect of A20 re-expression in KM-H2 cells on apoptosis, the difference in the fractions of Annexin-V-positive cells between Tet (+) and Tet (−) groups was also tested by a paired *t*-test for assays, in which the data from the assays performed on the same day were paired.

Histological and immunophenotypic changes in 59 cases of B-cell non-Hodgkin's lymphoma after rituximab therapy

Akiko Miyagi Maeshima,[1,4] Hirokazu Taniguchi,[1] Junko Nomoto,[2] Dai Maruyama,[2] Sung-Won Kim,[2] Takashi Watanabe,[2] Yukio Kobayashi,[2] Kensei Tobinai[2] and Yoshihiro Matsuno[3]

[1]Clinical Laboratory; [2]Hematology and Stem Cell Transplantation Divisions, National Cancer Center Hospital, Tokyo; [3]Department of Surgical Pathology, Hokkaido University Hospital, Sapporo, Japan

(Received June 30, 2008/Revised September 4, 2008/Accepted September 12, 2008/Online publication November 25, 2008)

Rituximab is a chimeric monoclonal antibody that recognizes the CD20 antigen. It has been used to treat B-cell non-Hodgkin lymphoma (B-NHL), but recently rituximab resistance has been a cause for concern. We examined histological and immunohistochemical changes in 59 patients with B-NHL after rituximab therapy. The patients comprised 32 men and 27 women with a median age of 59 years. Pre-rituximab specimens comprised 34 follicular lymphomas (FL), 11 diffuse large B-cell lymphomas (DLBCL), 10 mantle cell lymphomas, two marginal zone B-cell lymphomas (MZBCL), and two chronic lymphocytic leukemias (CLL). CD20 expression in lymphoma cells was evaluated by immunohistochemistry or flow cytometry. Post-rituximab materials were taken a median of 6 months (4 days to 59 months) after rituximab therapy. Sixteen cases (27%) showed loss of CD20 expression with four histological patterns: pattern 1, no remarkable histological change (FL, 5; DLBCL, 3; and CLL, 2); pattern 2, proliferation of plasmacytoid cells (FL, 2; DLBCL, 1; and MZBCL, 1); pattern 3, transformation to classical Hodgkin's lymphoma (FL, 1); and pattern 4, transformation to anaplastic large cell lymphoma-like undifferentiated lymphoma (FL, 1). Loss of CD20 was unrelated to the interval of biopsies, treatment regimen, clinical response, and frequency of rituximab administration. Loss of CD20 within 1 month of rituximab therapy (3/14, 21%) and regain of CD20 (2/7, 29%) were not frequent. CD20-positive relapse with transformation occurred most frequently in cases of early relapse. In conclusion, B-NHL showed various histological and immunophenotypic changes after rituximab therapy, including not only CD20 loss but also proliferation of plasmacytoid cells or transformation to special subtypes of lymphoma. (*Cancer Sci* 2009; 100: 54–61)

Rituximab is a chimeric monoclonal antibody that has recently been incorporated into the treatment of B-cell non-Hodgkin lymphoma (B-NHL). It recognizes the CD20 antigen, a pan-B-cell marker, binds to it, and induces apoptosis of CD20-positive cells.[1–4] Rituximab can be used as a monotherapy or in combination with conventional chemotherapy for treatment of low- and high-grade, untreated, relapsed, or refractory CD20-positive B-NHL, achieving a high response rate with a low toxicity.

Recent studies have reported that B-NHL show CD20-negative relapse after rituximab therapy.[5–17] Transformation of follicular lymphoma (FL) to CD20-negative diffuse large B-cell lymphoma (DLBCL),[15] proliferation of CD20-negative plasmacytoid tumor cells of marginal zone B-cell lymphoma (MZBCL)[16] or lymphoplasmacytic lymphoma,[13] transformation of FL to classical Hodgkin's lymphoma,[17] and progression of nodular lymphocyte-predominant Hodgkin lymphoma to CD20-negative T-cell-rich B-cell lymphoma have also been reported.[18]

Several mechanisms of resistance to rituximab have been suggested, including selection of a CD20-negative clone as a consequence of rituximab exposure, masking of CD20 epitopes by rituximab itself, or true loss of CD20 antigen by genetic and epigenetic changes.[12,13,15,19–24]

In the present study we carried out retrospective analyses of histological and immunophenotypic changes and outcome in 59 patients with B-NHL after rituximab-containing therapy, to explore the effect of rituximab on CD20 expression and morphology in B-NHL.

Materials and Methods

Patient selection. We reviewed the pathology archives of the National Cancer Center Hospital, Tokyo, Japan, for the period 2002 to 2007. Fifty-nine consecutive cases of CD20-positive B-NHL treated with rituximab, with or without chemotherapy, for which pre- and post-rituximab specimens were available, were included in our study. Rituximab (Zenyaku Kogyo, Tokyo, Japan) was used at a standard dose of 375 mg/m^2 once a week for rituximab monotherapy and once every 3 weeks for the rituximab-cyclophosphamide, doxorubicin, vincristine and prednisone (CHOP) regimen. Clinical information was extracted from the medical records, and the Ann Arbor system was used for staging.

Histological review. Biopsy or surgical specimens were fixed in 10% neutral-buffered formalin overnight, embedded in paraffin, cut into sections 4 μm thick, and stained with hematoxylin–eosin for histological evaluation. All of the pre-rituximab specimens were CD20-positive B-NHL by definition, and post-rituximab specimens included any lymphomas. All of the specimens were reviewed by three pathologists (A.M.M., H.T., and Y.M.) to confirm that the morphological characteristics fulfilled the criteria of the World Health Organization classification of lymphoid neoplasms, 2001.[25] Histological subtype, loss of CD20 expression by immunohistochemistry or flow cytometry, presence or absence of plasmacytoid differentiation, and the relationship between histological transformation and CD20 loss were examined.

Immunohistochemistry, flow cytometry, *in situ* hybridization, and interphase fluorescence *in situ* hybridization analyses. We carried out immunohistochemical staining on formalin-fixed paraffin-embedded pre- and post-rituximab specimens using a panel of monoclonal and polyclonal antibodies. Sections 4 μm thick were cut from each paraffin block, deparaffinized, and incubated

[4]To whom correspondence should be addressed. E-mail: akmaeshi@ncc.go.jp

doi: 10.1111/j.1349-7006.2008.01005.x

at 121°C in pH 6.0 citrate buffer for 10 min for antigen retrieval. Antibodies included those against the following antigens: CD3 (clone PS1, ×25; Novocastra, Newcastle, UK; polymer method), CD20 (L26, ×100; Dako, Glostrup, Denmark; labeled streptavidin–biotin method [LSAB]), and CD79a (JCB117, ×100; Dako; LSAB) routinely; and CD5 (4C7, ×50, Novocastra; polymer), CD7 (CD7-272, ×100; Novocastra; avidin–biotin complex method [ABC]), CD10 (56C6, ×50; Novocastra; polymer), CD15 (MMA, ×100; Becton Dickinson, Franklin Lakes, NJ, USA; polymer), CD30 (Ber-H2, ×100; Dako; polymer), CD45 (2B11 + PD7/26, ×100; Dako; LSAB), CD45RO (UCHL1, ×50; Dako; LSAB), CD56 (1B6, ×100; Novocastra; LSAB), ALK (ALK1, ×200; Dako; polymer), Bcl-2 (124, ×100; Dako; LSAB), Bcl-6 (poly, ×50; Dako; ABC), cyclin D1 (SP4, ×25; Nichirei, Tokyo, Japan; polymer), TIA-1 (26gA10F5, ×1000; Immunotech, Marseille, France; polymer), granzyme B (GrB-7, ×200; Dako; polymer), MPO (poly, ×1000; Dako; LSAB), MUM1 (MUM1p, ×50; Dako; ABC), PAX5 (24, ×200; Becton Dickinson; ABC), TdT (poly, ×100; Dako; polymer), Ig (poly, ×20 000; Dako; LSAB), Ig (poly, ×40 000; Dako; LSAB), IgA (poly, ×100 000; Dako; polymer), IgG (poly, ×20 000; Dako; polymer), and IgM (poly, ×20 000; Dako; polymer) optionally. The percentages of CD20-positive tumor cells were counted semiquantitatively by immunohistochemistry (IHC). Immunoreactivity for CD20 was judged positive (no CD20 loss) if >95% of the tumor cells were stained, partially negative (partial CD20 loss) if 10–95% of the cells were stained, or negative (CD20 loss) if <10% of the cells were stained. When a post-rituximab specimen showed loss of CD20 expression, it was judged as B-cell lineage if there was positivity for CD79a.

Flow cytometry was carried out using an Epics XL-MCL instrument with System II Software (Beckman Coulter). The flow cytometry panel included CD20 (B-Ly1), CD19 (HD37), Ig (poly), and Ig (poly) (Dako). Fluorescence *in situ* hybridization (FISH) and *in situ* hybridization (ISH) analyses were optional. Sections 4 μm thick were cut from each paraffin block and used for FISH analysis. Judgment of the fusion gene was carried out as described previously.[26] Dual-color LSI IGH Spectrum Green/LSI BCL2 Spectrum Orange Dual Fusion Translocation Probes (Vysis, Downers Grove, IL, USA) were used to detect t(14;18): IGHBCL2 fusion. ISH with Epstein–Barr-encoded RNA (EBER-1) probes (Dako) was carried out in some cases to detect possible Epstein–Barr virus infection.

Statistical analysis. The relationships between CD20 expression and treatment regimen (rituximab monotherapy vs combination therapy with rituximab and chemotherapy), response (complete response [CR] vs others, or overall response [OR] vs others), frequency of rituximab administration, and interval between the last dose of rituximab and rebiopsy were examined by ^{2}-test or Mann-Whitney *U*-test. Differences were considered significant when the *P*-value was less than 0.05.

Results

Patient characteristics. Clinical information for all consecutive 59 patients is summarized in Table 1. The patients comprised 32 men and 27 women, ranging in age from 37 to 80 years with a median age of 59 years. Eight patients had stage I/II disease and 51 patients had stage III/IV disease. All of the patients received rituximab by definition, with or without chemotherapy (CHOP or other types of regimen). The 59 patients received a median of six courses (range 1–17) of rituximab. The median interval between the last dose of rituximab and rebiopsy was 6 months (range 4 days to 59 months). The overall response rate was 79% and the % CR was 46% to rituximab-containing regimens.

Four histological patterns of CD20 loss. The results of histological analysis and immunohistochemical staining for each antibody are summarized in Tables 1–2. The total of 59 pre-rituximab B-NHL specimens included 34 FL with or without a DLBCL component, 11 DLBCL, 10 mantle cell lymphomas (MCL), two MZBCL, and two chronic lymphocytic leukemias (CLL). We considered that the following two factors may have contributed to case selection bias. The first factor is that the date of the approval of rituximab for low-grade B-cell lymphoma preceded that for DLBCL for 2 years in Japan. The second factor is that FL were rebiopsied more frequently than DLBCL because FL relapsed frequently and were followed up for a long time, and checks for transformation to DLBCL were sometimes necessary.

Sixteen cases (27%) showed loss of CD20 expression in post-rituximab specimens by IHC or flow cytometry. The frequencies of CD20 loss in the various histological subtypes were: FL, 26% (9/34); DLBCL, 36% (4/11); MCL, 0% (0/10); MZBCL, 50% (1/2); and CLL, 100% (2/2). Among them, two DLBCL and two FL showed partial loss of CD20 expression. Among the 12 tumors with complete loss of CD20 expression, seven had available flow cytometry data, and all of them showed loss of CD20.

Four patterns of loss of CD20 expression were evident (Table 2): pattern 1, CD20 loss with no remarkable histological change (FL, 5; DLBCL, 3; and CLL, 2) (Fig. 1); pattern 2, proliferation of plasmacytoid cells (FL, 2; DLBCL, 1; and MZBCL, 1) (Fig. 2); pattern 3, transformation to classical Hodgkin lymphoma (FL, 1); and pattern 4, transformation to anaplastic large cell lymphoma (ALCL)-like undifferentiated lymphoma (FL, 1) (Fig. 3). All of the lymphomas after rituximab treatment with pattern 1 or 2 histology were positive for CD79a. Two FL with pattern 2 showed proliferation of plasmacytoid cells, not in the marginal zone but in follicles, as with FL with plasma cells,[27,28] and the plasmacytoid tumor cells were positive for IgM and Ig by IHC. One DLBCL with pattern 2 was negative for IgM and Ig by IHC in the pre-rituximab specimen, but positive for them in the post-rituximab specimen. Hodgkin lymphoma with pattern 3, which was previously reported to be a form of transformed FL,[29] was positive for CD30, CD15, and the IGH–BCL2 fusion by FISH, and negative for CD10, CD20, and EBER-1 by ISH. Although we could not determine the lineage of ALCL-like undifferentiated lymphoma with pattern 4, because it was positive for only CD45 and CD45RO and negative for CD3, CD5, CD7, CD10, CD15, CD20, CD30, CD56, CD79a, ALK, bcl-2, bcl-6, granzyme B, MPO, MUM1, PAX5, TdT, TIA-1, and EBER-1 by ISH, it was considered to be transformed FL because of the presence of the IGHBCL2 fusion revealed by FISH in both the pre- and post-rituximab specimens (Fig. 3).

Relationship between rituximab therapy and CD20 expression, and histological changes. The relationships between CD20 expression and interval after the last dose of rituximab, treatment regimens, clinical response, and frequency of rituximab administration were not detected. Among 16 cases showing loss of CD20, the clinical response to treatment was no change (NC) in three cases, and CR or partial response (PR) in the others.

Fourteen patients underwent rebiopsy within 1 month of the last dose of rituximab. Among them, only three cases (21%) were negative for CD20. Seven cases showing loss of CD20 expression after rituximab therapy were subsequently observed and rebiopsied and, among them, two cases (cases FL4-2 and FL8) regained CD20 expression at 7 and 15 months after the last dose of rituximab. The other five cases were found not to have regained CD20 expression at 2, 7, 12, 28, and 44 months after the last dose of rituximab.

Nine patients with FL achieved CR or PR after treatment with a rituximab-containing regimen, but their lymphomas showed early relapse (within 3 months to 1 year later). Among them, five cases (cases FL12, FL18, FL25, FL33, and FL34) relapsed as CD20-positive DLBCL, two (cases FL16 and FL21) as CD20-positive low-grade FL, one (case FL3-2) as CD20-negative FL grade 2, and one (case FL8) as transformation to Hodgkin's lymphoma.

Table 1. Patient characteristics

Case	Age (years)/sex	Stage	Pre-rituximab diagnosis (sample)	Therapy and response between biopsy and operation	Post-rituximab diagnosis (sample)	Post-rituximab interval (months)†	CD20 expression (%)	Histology by immunohistochemistry	Pattern
FL1	55/M	4	FL, gr.2 (LN)	Rx4, NC	FL, gr.1 (BM)	3	0	NHC	1
FL2	52/M	4	FL, gr.2 (LN)	C-MOPPx8, PR, Rx4, NC	FL, gr.1 (BM)	22	0	NHC	1
FL3-1	52/M	3	FL, gr.1 (LN)	R-CHOPx6, CR	FL, gr.2 (BM)	33	100	NHC	
FL3-2				Rx8+C-MOPPx5, CR, relapse, R-ICEx2, PR	FL, gr.2 (LN)	6	0	NHC	1
FL4-1	42/F	4	FL, gr.1 (LN)	Rx8+C-MOPPx16, NC	FL, gr.1 (BM)	23	100	NHC	
FL4-2				Rx8, NC	FL, gr.1 (BM)	5 days	0	NHC	1
FL5	59/M	4	FL, gr.2 (LN)	Rx4, NC, C-MOPPx13, PD, R-C-MOPPx8, CR	FL, gr.2 (BM)	21	–‡	NHC	1
FL6	40/M	4	FL, gr.1 (LN)	R-CHOPx6, CR	FL, gr.2 (LN)	12	90	Partially plasmacytoid cells (IgM+/Ig +/CD138–)	2
FL7	49/F	4	FL, gr.1 (duodeunum)	R-CHOPx6, CR	FL, gr.1 (LN)	17	90	Partially plasmacytoid cells (IgM+/Ig +/CD138–)	2
FL8	61/F	4	DLBCL+FL, gr.3a (LN)	Rx4+CHOPx8, CR	HL, MC (LN)	11	0	Transformation to HL	3
FL9	68/M	4	FL, gr.2 (LN)	R-C-MOPPx6, R-C-MOPPx8, relapse, fludarabine + Rx3	ALCL-like (liver)	18 days	0	Transformation to ALCL-like	4
L10	76/F	4	FL, gr.2 (LN)	Rx8, NC	FL, gr.2 (BM)	6	100	NHC	
FL11	54/F	4	FL, gr.2 (LN)	R-CHOPx6, CR	FL, gr.1 (BM)	15 days	100	NHC	
FL12	40/F	4	FL, gr.1 (LN)	CHOPx6, CR, relapse, C-MOPPx4, NC, Rx4, CR	DLBCL (colon)	4	100	Transformation to DLBCL	
FL13	44/M	4	FL, gr.2 (LN)	R-CHOPx6, PR, C-MOPPx6 radiation, PR	DLBCL+FL, gr.1 (BM)	59	100	Transformation to DLBCL	
FL14	47/M	4	FL, gr.2 (LN)	COPPx6, NC, Rx4, PD	FL, gr.1 (BM)	1	100	NHC	
FL15	43/M	4	FL, gr.1 (LN)	Rx4+C-MOPPx2, CR, zevalin, CR	FL, gr.1 (orbit)	26	100	NHC	
FL16	61/F	4	FL, gr.1 (BM), DLBCL (skin)	R-CHOPx8, CR	FL, gr.2 (LN)	9	100	NHC	
FL17	48/F	4	FL, gr.2 (LN)	Rx4+CHOPx6, PR	FL, gr.1 (BM)	23	100	NHC	
FL18	60/F	3	FL, gr.2 (LN)	Rx4, CR	DLBCL (tonsil)	4	100	Transformation to DLBCL	
FL19	54/F	4	FL, gr.1 (BM, stomach)	R-CHOPx6, PR	FL, gr.1 (BM)	37	100	NHC	
FL20	54/F	4	FL, gr.1 (LN)	Rx4, PR, CHOPx8, PR	FL, gr.2 (cecum)	36	100	NHC	
FL21	61/F	4	FL, gr.2 (LN)	R-CHOPx8, PR	FL, gr.1 (BM)	5	100	NHC	
FL22	66/F	3	FL, gr.2 (LN)	R-CHOPx8, PR	FL, gr.2 (skin)	26	100	NHC	
FL23	53/F	4	FL, gr.2 (ileum, colon)	R-CHOPx8, NC	FL, gr.1 (duodenum)	10	100	NHC	
FL24	51/F	4	FL, gr.2 (duodenum)	Rx1 (within R-CHOP)	FL, gr.1 (duodenum)	4 day	100	NHC	
FL25	55/M	3	DLBCL+FL, gr.3b (LN)	R-CHOPx8, CR	DLBCL (LN)	3	100	NHC	
FL26	37/M	4	FL, gr.2 (LN)	Rx2 (within R-CHOP)	FL, gr.2 (duodenum)	8 days	100	NHC	
FL27	62/M	4	FL, gr.1 (ileum)	Rx3 (within R-CHOP)	FL, gr.1 (duodenum)	8 days	100	NHC	
FL28	57/F	4	FL, gr.3a (LN)	Rx4, NC	DLBCL (LN)	3	100	Transformation to DLBCL	
FL29	51/M	3	DLBCL+FL, gr.3b (LN)	R-CHOPx6+Rx8, CR	DLBCL (LN)	21 days	100	NHC	
FL30	60/M	1	FL, gr.1 (duodenum)	Rx8, CR	FL, gr.1 (duodenum)	4 days	100	NHC	
FL31	63/M	1	FL, gr.1 (duodenum)	Rx8, PR	FL, gr.1 (duodenum)	1	100	NHC	
FL32	75/F	4	FL, gr.1 (BM)	Rx3	FL, gr.1 (BM)	4 days	100	NHC	
FL33	77/M	4	DLBCL+FL, gr.3a (pharynx)	R-CHOPx8, CR	DLBCL (LN)	8	100	NHC	

doi: 10.1111/j.1349-7006.2008.01005.x

Table 1. Continued

Case	Age (years)/sex	Stage	Pre-rituximab diagnosis (sample)	Therapy and response between biopsy and operation	Post-rituximab diagnosis (sample)	Post-rituximab interval (months)†	CD20 expression (%)	Histology by immunohistochemistry	Pattern
FL34	65/M	3	FL, gr.3a (LN)	Rx8, CR	DLBCL (LN)	5	100	Transformation to DLBCL	
DLBCL1-1	47/M	2	DLBCL (right testis)	R-CHOPx8, CR	DLBCL (left testis)	2	100	NHC	
DLBCL1-2				R-IVACx3, CR, BMT, CR	DLBCL (BM)	4	0	NHC	1
DLBCL2	71/M	3	DLBCL (ileum)	R-CHOPx8, CR, Rx1	DLBCL (LN)	10 days	10	NHC	1
DLBCL3	55/M	4	DLBCL (tonsil)	R-CHOPx8, PR	DLBCL (LN)	3	70	NHC	1
DLBCL4	58/F	2	DLBCL (EBER-1+) (stomach)	R-CHOPx8, PR	DLBCL (stomach)	4	0	Plasmacytoid cells (IgM+/Ig +/CD138–)	2
DLBCL5	80/M	2	DLBCL (LN)	R-CHOPx8, CR	DLBCL (subcutaneous)	6	100	NHC	
DLBCL6	60/F	4	DLBCL (breast)	Chemotherapy, Rx4, CR	DLBCL (breast)	29 days	100	NHC	
DLBCL7	61/F	2	DLBCL (tonsil)	R-EPOCHx4, CR	DLBCL (colon, rectum)	16	100	NHC	
DLBCL8	75/F	4	DLBCL (stomach,duodenum)	R-CHOPx8, CR	DLBCL (stomach, duodenum)	30	100	NHC	
DLBCL9	65/F	3	DLBCL (LN)	Rx8+CHOPx6, PD	DLBCL (LN)	3	100	NHC	
DLBCL10	64/M	2	DLBCL (stomach)	Rx1+CHOPx2 (within R-CHOP)	DLBCL (stomach)	20 days	100	NHC	
DLBCL11	63/M	2	DLBCL (LN)	Rx8+CHOPx5+radiation, CR	DLBCL (LN)	8	100	NHC	
MCL1	72/M	4	MCL (LN)	R-CHOPx4, PR, Rx4, NC, COPx6, PD, R-CNOPx6, PD, cladribine, PD	MCL (stomach)	10 days	100	NHC	
MCL2	76/M	4	MCL (LN)	R-CHOPx8, PR	MCL (BM)	20	100	NHC	
MCL3	68/M	4	MCL (BM)	Rx1+CHOPx6, PR	MCL (BM)	1	100	NHC	
MCL4	66/M	4	MCL (colon)	R-CHOPx8, CR	MCL (stomach)	30	100	NHC	
MCL5	55/M	4	MCL (tonsil)	Rx4, PR	MCL (tongue)	28	100	NHC	
MCL6	59/F	4	MCL (stomach)	Rx4, PR, C-MOPPx8+ radiation+COP, PD	MCL (bone)	21	100	NHC	
MCL7-1	63/F	4	MCL (LN)	Rx4+C-MOPPx8, CR	MCL (stomach, duodenum)	17	100	NHC	
MCL7-2				Rx4, PR	MCL (stomach)	1	100	NHC	
MCL8	54/F	4	MCL (ileum)	Rx8+CHOPx6, CR	MCL (small intestine)	3	100	NHC	
MCL9	78/M	4	MCL (stomach)	Rx8, PD	MCL (orbit)	2	100	Change to blastoid variant	
MCL10	70/M	4	MCL (LN)	R-CHOPx8, PR	MCL (stomach)	18	100	NHC	
MZBCL1	68/F	3	MZBCL (LN)	R-ICEx1, CR	MZBCL (tonsil)	15	0	Plasmacytoid cells	2
MZBCL2	55/M	4	MZBCL (BM)	R-CHOPx6, PR	MZBCL (BM)	4	100	NHC	
CLL1	54/M	4	CLL (BM)	Rx2+C-MOPPx6, PR	CLL (LN)	12 days	0	NHC	1
CLL2	52/F	4	CLL (BM)	CHOPx8, COPx10, R-CEPPx7, R-ESHAPx2, CHASEx2, R-ESHAP+PBSCT, Rx5, PR	CLL (BM)	11	0	NHC	1

†From last dose of rituximab; ‡by flow cytometry. ALCL, anaplastic large cell lymphoma; BM, bone marrow; BMT, bone marrow transplantation; CEPP, cyclophosphamide, etoposide, procarbazine, and prednisolone; CHASE, cyclophosphamide, cytosine arabinoside, etoposide, and dexamethasone; CHOP, cyclophosphamide, doxorubicin, vincristine, and prednisone; CLL, chronic lymphocytic leukemia; C-MOPP, cyclophosphamide, vincristine, prednisone, and procarbazine; CR, complete response; diff., differentiation; DLBCL, diffuse large B-cell lymphoma; EPOCH, etoposide, prednisone, vincristine, cyclophosphamide, and doxorubicin; ESHAP, etoposide, methylprednisolone, high-dose cytarabine, and cisplatin; FL, follicular lymphoma; HL, Hodgkin's lymphoma; ICE, ifosfamide, carboplatin, and etoposide; IVAC, ifosfamide, vincristine, and cytarabine; LN, lymph node; MC, mixed cellularity; MCL, mantle cell lymphoma; MZBCL, marginal zone B-cell lymphoma; NC, no change; NHC, no remarkable histological change; PBSCT, peripheral blood stem cell transplantation; PD, progressive disease; PR, partial response; R, rituximab.

Cancer Sci | January 2009 | vol. 100 | no. 1 | 57

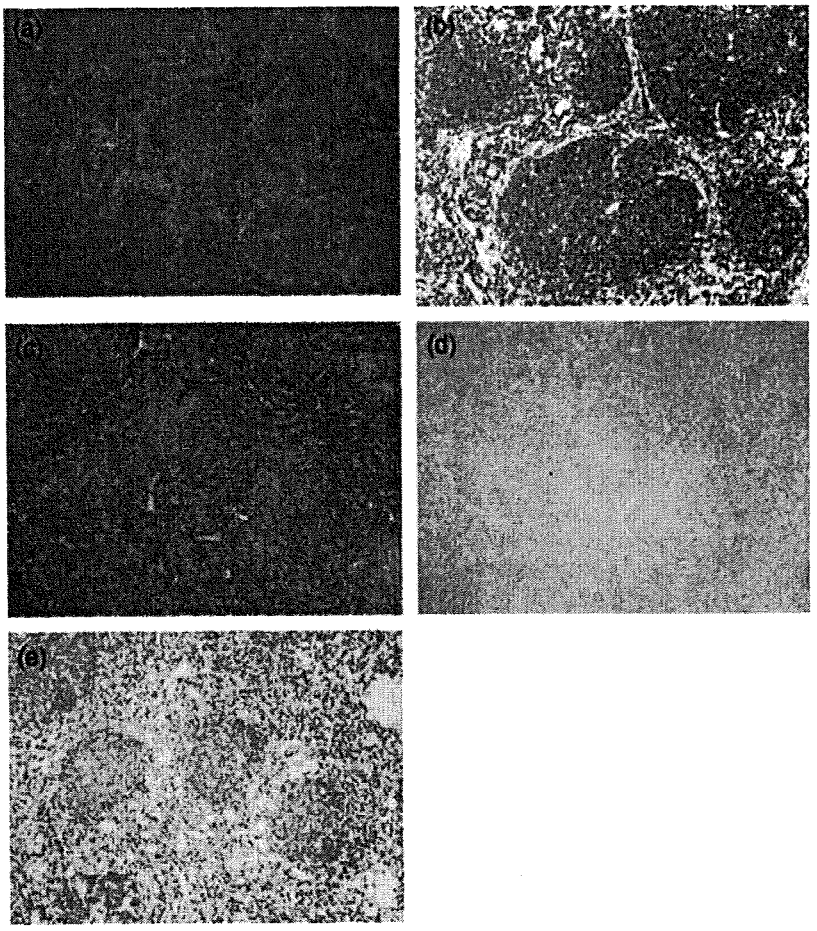

Fig. 1. (a–e) A case of pattern 1 change in CD20-positive follicular lymphoma (FL) to CD20-negative FL. FL, grade 1, (a) in a lymph node (hematoxylin–eosin, ×40) and (b) with CD20-positive phenotype, pre-rituximab (×100). FL, grade 2, (c) in a lymph node (hematoxylin–eosin, ×40) with (d) CD20-negative (×40) and (e) CD79a-positive (×40) phenotypes, post-rituximab.

Table 2. Four histological patterns of loss of CD20 expression after rituximab therapy

Histological pattern	Distribution
Pattern 1: loss of CD20 with no remarkable histological change	FL, 5; DLBCL, 3; CLL, 2
Pattern 2: proliferation of plasmacytoid cells	FL, 2; DLBCL, 1; MZBCL, 1
Pattern 3: transformation to classical Hodgkin lymphoma	FL, 1
Pattern 4: transformation to anaplastic large cell lymphoma-like undifferentiated lymphoma	FL, 1

CLL, chronic lymphocytic leukemia; DLBCL, diffuse large B-cell lymphoma; FL, follicular lymphoma; MZBCL, marginal zone B-cell lymphoma.

Discussion

Recent reports have indicated that the treatment of B-NHL with rituximab may be associated with CD20-negative lymphoma relapse,[5–17] and the frequency of loss of CD20 after rituximab treatment varies widely (24, 56, 60, and 94%).[9,11,13,14] In the present study, 16 of 59 B-NHL (27%) showed loss of CD20 after rituximab-containing therapy using a larger series than in previous reports. Our results also suggested that the frequency of CD20 loss was not largely affected by the period before rebiopsy. Although the site of sampling (bone marrow vs non-bone marrow) might affect the observed degree of CD20 loss,[9] this issue needs to be studied further using a larger number of cases. Tumors with loss of CD20 in the present study included FL, DLBCL, MZBCL, and CLL. Although Goteri *et al.* reported that MCL frequently showed loss of CD20 expression in bone marrow, none of our MCL cases showed CD20 loss.[13] Because a previous report indicated that rituximab + CHOP combination therapy (R-CHOP) had insufficient efficacy for MCL,[30] it was considered that this regimen might not have been sufficiently potent to induce selection of a CD20-negative clone.

Four histological patterns of CD20 loss were evident. The majority were patterns 1 or 2, whereas patterns 3 or 4 were rare. Recently, several reports have described relapse with pattern 1 or 2 histology after rituximab therapy.[13,16] Using flow cytometry, Goteri *et al.* demonstrated that 26 cases of low-grade B-cell lymphoma showed CD20 loss in bone marrow aspirates, including cases with no histological change, and with residual plasmacytoid tumor cells of lymphoplasmacytic lymphoma.[13] It has also been reported that mucosa-associated lymphoid tissue lymphoma changes to a pure plasma-cell neoplasm.[16]

Case FL8, which showed transformation to Hodgkin lymphoma (pattern 3), was one of the transformed FL that we reported previously.[29] As composite Hodgkin lymphoma and FL is reported to be very rare,[31,32] rituximab might have induced transformation to Hodgkin lymphoma. Recently, a case

doi: 10.1111/j.1349-7006.2008.01005.x

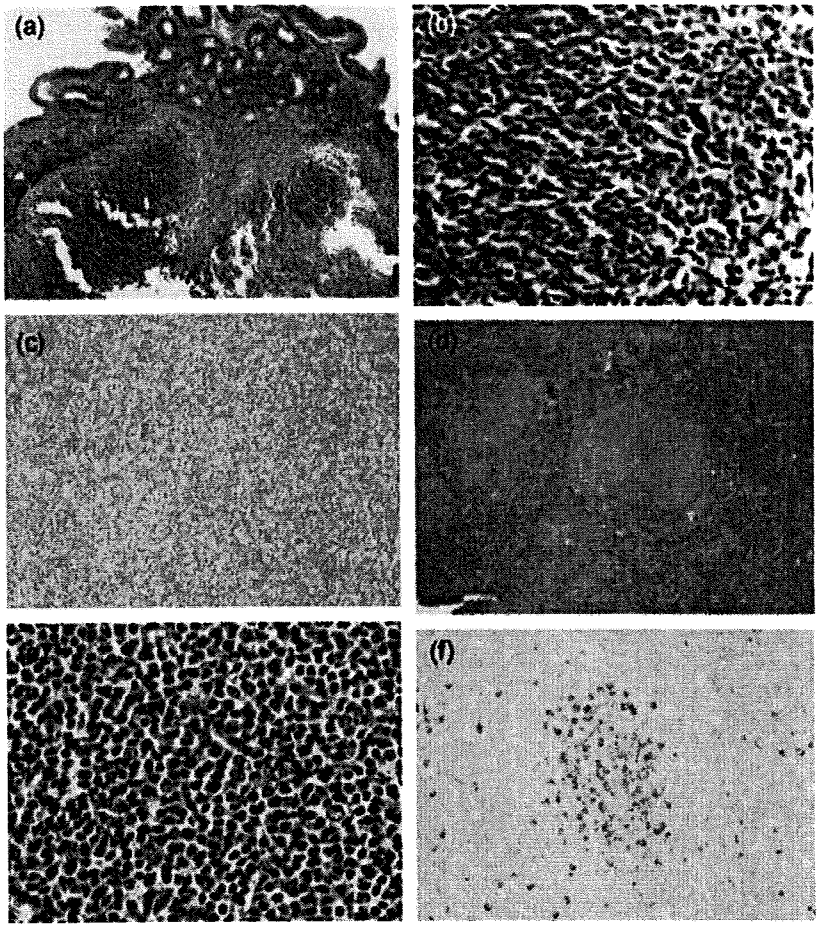

Fig. 2. (a–f) A case of pattern 2 change of follicular lymphoma (FL) to FL with plasma cells. FL, grade 1 in duodenum (hematoxylin–eosin), (a) ×40, (b) ×400, with (c) IgM-negative phenotype (×100), pre-rituximab. FL, grade 1 with plasmacytoid differentiation in lymph node (hematoxylin–eosin), (d) ×40, (e) ×400, with (f) IgM-positive phenotype (×100), post-rituximab.

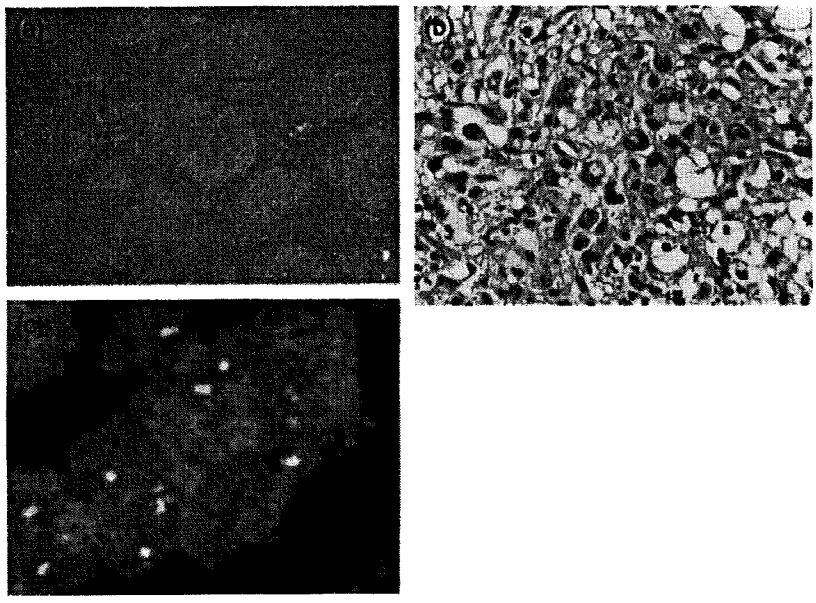

Fig. 3. (a–c) A case of pattern 4 change of follicular lymphoma (FL) to anaplastic large-cell lymphoma (ALCL)-like undifferentiated lymphoma. (a) FL, grade 2 in lymph node, pre-rituximab (hematoxylin–eosin, ×40). (b) ALCL-like undifferentiated lymphoma in liver, post-rituximab (hematoxylin–eosin, ×400). (c) The result of fluorescence *in situ* hybridization of ALCL-like undifferentiated lymphoma. IGH and BCL2 fusion pattern. Two fusion IGHBCL2 signals were present.

of Hodgkin lymphoma subsequent to FL in a patient receiving maintenance rituximab was reported.[17]

Transformation from FL to ALCL-like undifferentiated lymphoma (pattern 4) has been reported previously as neither transformation of FL nor histological change after rituximab therapy. Although two cases of FL with relapse to peripheral T-cell lymphoma after rituximab have been reported,[33,34] it was suspected that the T-cell lymphomas were another clone, thus differing from the present case. Cohen *et al.* reported large-cell transformation of CLL and FL during or soon after treatment with a fludarabine- and rituximab-containing regimen,[35] thus resembling the present case treated with fludarabine and rituximab.

Several mechanisms of resistance to rituximab have been suggested, including selection of a CD20-negative clone as a consequence of rituximab exposure, masking of CD20 epitopes by rituximab itself, or true loss of CD20 antigen due to genetic and epigenetic changes.[12,13,15,19–24] Although the present study was not intended to address the mechanism of CD20 loss, several remarkable phenomena were evident. No relationships were detected between loss of CD20 and the interval between the last dose of rituximab and rebiopsy, frequency of rituximab administration, clinical responses, and treatment regimens. It is suspected that susceptibility to rituximab differs greatly among lymphomas. Our results also indicated that loss of CD20 immediately after rituximab therapy was not frequent. Although some cases do regain CD20 expression, loss of CD20 persisting for more than 6 months is not infrequent.

A previous case report has emphasized that early relapse of FL after rituximab therapy was related to CD20-negative transformation to DLBCL.[15] However, this was not confirmed in our study using a larger series: most of the relapses were CD20-positive DLBCL, and only two were CD20-negative FL or Hodgkin lymphoma. Our results suggested that CD20-positive relapse with histological transformation occurred most frequently in cases of early relapse, and that CD20-negative relapse was relatively rare.

In conclusion, our findings indicate that 27% of B-NHL show loss of CD20 expression with four histological patterns after rituximab therapy. As the changes in morphology and CD20 expression after rituximab therapy vary widely, including not only loss of CD20 expression but also proliferation of plasmacytoid cells or transformation to special subtypes of lymphoma, and clinical outcomes are very confused, careful follow up and rebiopsy are recommended.

Acknowledgments

The authors are grateful to Ms S. Miura and Ms C. Kina for their excellent technical assistance.

References

1 Reff ME, Carner K, Chambers KS *et al.* Depletion of B cells *in vivo* by a chimeric mouse human monoclonal antibody to CD20. *Blood* 1994; 83: 435–45.
2 Demidem A, Lam T, Alas S *et al.* Chimeric anti-CD20 (IDEC-C2B8) monoclonal antibody sensitizes a B cell lymphoma cell line to cell killing by cytotoxic drugs. *Cancer Biother Radiopharm* 1997; 12: 177–86.
3 Shan D, Ledbetter JA, Press OW. Apoptosis of malignant human B cells by ligation of CD20 with monoclonal antibodies. *Blood* 1998; 91: 1644–52.
4 Cardarelli PM, Quinn M, Buckman D *et al.* Binding to CD20 by anti-B1 antibody or F(ab)(2) is sufficient for induction of apoptosis in B-cell lines. *Cancer Immunol Immunother* 2002; 51: 15–24.
5 Meeker T, Lewder J, Cteary ML *et al.* Emergence of idiotype variants during treatment of B-cell lymphoma with anti-idiotype antibodies. *N Eng J Med* 1985; 312: 1658–65.
6 Kinoshita T, Nagai H, Murate T *et al.* CD20-negative relapse in B-cell lymphoma after treatment with rituximab. *J Clin Oncol* 1998; 16: 3916.
7 Davis TA, Czerwinski DK, Levy R. Therapy of B-cell lymphoma with anti-CD20 antibodies can result in the loss of CD20 antigen expression. *Clin Cancer Res* 1999; 5: 611–15.
8 Schmitz K, Brugger W, Weiss B *et al.* Clonal selection of CD20-negative non-Hodgkin's lymphoma cells after treatment with anti-CD20 antibody rituximab. *Br J Haematol* 1999; 106: 571–2.
9 Foran JM, Norton AJ, Micallef IN *et al.* Loss of CD20 expression following treatment with rituximab (chimaeric monoclonal anti-CD20): a retrospective cohort analysis. *Br J Haematol* 2001; 114: 881–3.
10 Chu PG, Chen YY, Molina A *et al.* Recurrent B-cell neoplasms after Rituximab therapy: an immunophenotypic and genotypic study. *Leuk Lymphoma* 2002; 43: 2335–41.
11 Kennedy GA, Tey SK, Cobcroft R *et al.* Incidence and nature of CD20-negative relapses following rituximab therapy in aggressive B-cell non-Hodgkin's lymphoma: a retrospective review. *Br J Haematol* 2002; 119: 412–16.
12 Jilani I, O'Brien S, Manshuri T *et al.* Transient down-modulation of CD20 by rituximab in patients with chronic lymphocytic leukemia. *Blood* 2003; 102: 3514–20.
13 Goteri G, Olivieri A, Ranaldi M *et al.* Bone marrow histopathological and molecular changes of small B-cell lymphomas after rituximab therapy: comparison with clinical response and patients' outcome. *Int J Immunopathol Pharmacol* 2006; 19: 421–31.
14 Seliem RM, Freeman JK, Steingart RH *et al.* Immunophenotypic changes and clinical outcome in B-cell lymphomas treated with rituximab. *Appl Immunohistochem Mol Morphol* 2006; 14: 18–23.
15 Alovaro-Naranjo TA, Jaen-Martinez JJ, Guma-Padro JG *et al.* CD20-negative DLBCL transformation after rituximab treatment in follicular lymphoma: a new case report and review of the literature. *Ann Hematol* 2003; 82: 585–8.
16 Woehrer S, Streubel B, Chott A *et al.* Transformation of MALT lymphoma to pure plasma cell histology following treatment with the anti-CD20 antibody rituximab. *Leuk Lymphoma* 2005; 46: 1645–9.
17 Scaramucci L, Perrotti A, Niscola P *et al.* Hodgkin disease subsequent to follicular lymphoma on maintenance rituximab. *Leuk Lymphoma* 2007; 48: 1878–80.
18 Pijuan L, Vicioso L, Bellosillo B *et al.* CD20-negative T-cell-rich B-cell lymphoma as a progression of a nodular lymphocyte-predominant Hodgkin's lymphoma treated with rituximab: a molecular analysis using laser capture microdissection. *Am J Surg Pathol* 2005; 29: 1399–403.
19 Cragg MS, Bayne MC, Illidge TM *et al.* Apparent modulation of CD20 by rituximab: an alternative explanation. *Blood* 2004; 103: 3989–90.
20 Rawal YB, Nuovo GJ, Frambach GE *et al.* The absence of CD20 messenger RNA in recurrent cutaneous B-cell lymphoma following rituximab therapy. *J Cutan Pathol* 2005; 32: 616–21.
21 Takei K, Yamazaki T, Sawada U *et al.* Analysis of changes in CD20, CD55, and CD59 expression on established rituximab-resistant B-lymphoma cell lines. *Leuk Res* 2006; 30: 625–31.
22 Tomita A, Hiraga J, Kiyoi H *et al.* Epigenetic regulation of CD20 protein expression in a novel B-cell lymphoma cell line, RRBL1, established from a patient treated repeatedly with rituximab-containing chemotherapy. *Int J Hematol* 2007; 86: 49–57.
23 Jazirehi AR, Vega MI, Bonavida B. Development of rituximab-resistant lymphoma clones with altered cell signaling and cross-resistance to chemotherapy. *Cancer Res* 2007; 67: 1270–81.
24 Czuczman MS, Olejniczak S, Gowda A *et al.* Acquirement of rituximab resistance in lymphoma cell lines is associated with both global CD20 gene and protein down-regulation regulated at the pretranscriptional and posttranscriptional levels. *Clin Cancer Res* 2008; 14: 1561–70.
25 Jaffe ES, Harris NL, Stein H *et al. World Health Organization Classification of Tumours Pathology & Genetics: Tumours of Haematopoietic and Lymphoid Tissues*. Lyon: IARC Press, 2001.
26 Sekiguchi N, Kobayashi Y, Yokota Y *et al.* Follicular lymphoma subgrouping by fluorescence *in situ* hybridization analysis. *Cancer Sci* 2005; 96: 77–82.
27 Keith TA, Cousar JB, Glick AD *et al.* Plasmacytic differentiation in follicular center cell (FCC) lymphomas. *Am J Clin Pathol* 1985; 84: 283–90.
28 Vago JF, Hurtubise PE, Redden-Borowski MM *et al.* Follicular center-cell lymphoma with plasmacytic differentiation, monoclonal paraprotein, and peripheral blood involvement: recapitulation of normal B-cell development. *Am J Surg Pathol* 1985; 9: 764–70.
29 Maeshima AM, Omatsu M, Nomoto J *et al.* Diffuse large B-cell lymphoma after transformation from low-grade follicular lymphoma: morphological, immunohistochemical and FISH analyses. *Cancer Sci* 2008; 99: 1760–8.
30 Lenz G, Dreyling M, Hoster E *et al.* Immunochemotherapy with rituximab and cyclophosphamide, doxorubicin, vincristine, and prednisone significantly improves response and time to treatment failure, but not long-term outcome in patients with previously untreated mantle cell lymphoma: results of a

doi: 10.1111/j.1349-7006.2008.01005.x

prospective randomized trial of the German Low Grade Lymphoma Study Group (GLSG). *J Clin Oncol* 2005; **23**: 1984–92.
31 Brauninger A, Hansmann ML, Strickler JG *et al.* Identification of common germinal-center B-cell precursors in two patients with both Hodgkin's disease and non-Hodgkin's lymphoma. *N Eng J Med* 1999; **340**: 1239–47.
32 Marafioti T, Hummel M, Anagnostopoulos I *et al.* Classical Hodgkin's disease and follicular lymphoma originating from the same germinal center B cell. *J Clin Oncol* 1999; **17**: 3804–9.
33 Micallef IN, Kirk A, Norton A *et al.* Peripheral T-cell lymphoma following rituximab therapy for B-cell lymphoma. *Blood* 1999; **93**: 2427–8.
34 Tetreault S, Abler SL, Robbins B *et al.* Peripheral T-cell lymphoma after anti-CD20 antibody therapy. *J Clin Oncol* 1998; **16**: 1635–7.
35 Cohen Y, Da'as N, Libstet D *et al.* Large-cell transformation of chronic lymphocytic leukemia and follicular lymphoma during or soon after treatment with fludarabine-rituximab-containing regimens: natural history- or therapy-related complication? *Eur J Haematol* 2002; **68**: 80–3.